Bachelor's thesis

Bio- ja Kemiantekniikka

2024

Karri Meriläinen

Non-contact bioleaching of black mass from waste lithium-ion batteries

TURKU AMK
TURKU UNIVERSITY OF APPLIED SCIENCES

Bachelor's Thesis | Abstract

Turku University of Applied Sciences

Biotechnology and Chemical Engineering

2024 | 50 pages

Karri Meriläinen

Non-contact bioleaching of black mass from waste lithium-ion batteries

The thesis aimed to investigate the viability of non-contact bioleaching in lithium-ion battery (LIB) recycling in the FuLIBatteR project. A total of four experiments were conducted, whereby the first two experiments investigated different pulp densities with four different battery types. The following two experiments studied how catalysts affect leaching, focusing solely on one LIB type having lithium nickel manganese cobalt oxides (NMC) as cathode material.

Bacteria-produced sulphuric acid was used for the leaching experiments of this thesis. Successful leaching was observed through pH and redox changes and leaching efficiencies were calculated from inductively coupled plasma optical emission spectrophotometry and a scanning electron microscope with elemental analysis.

The results indicated that non-contact leaching is a potential method in lithium-ion battery recycling. Leaching experiments were successful with high pulp densities and fast experimental times. Catalysts are not needed in leaching lithium and manganese, although it is necessary to leach cobalt. High catalyst concentrations proved to be detrimental to some metals due to precipitations. Combined catalyst usage was found to be unnecessary and future studies need to be carefully evaluated. The results should be confirmed as the sample sizes were low, and experimental errors were observed.

Future studies can be conducted based on these findings by further increasing pulp density, testing different battery types, or, e.g., utilizing ultra-sound in the leaching process.

Keywords:

bioleaching, recycling, lithium-ion batteries, non-contact, NMC

Opinnäytetyö (AMK) | Tiivistelmä

Turun ammattikorkeakoulu

Bio- ja kemiantekniikka

2024 | 50 sivua

Karri Meriläinen

Käytettyjen litiumioniakkujen arvokkaiden metallien epäsuora bioliuotus

Opinnäytetyössä tutkittiin epäsuoran bioliuotuksen soveltuvuutta litiumioniakkujen kierrätykseen osana FuLIBatteR-projektia. Kahdessa kokeessa tutkittiin neljää akkutyyppiä sekä kahta eri massatiheyttä. Onnistuneiden laboratoriokokeiden pohjalta toteutettiin vielä kaksi lisätestiä, joissa tutkittiin katalyyttien vaikutusta liuotukseen, kuitenkin keskittyen vain nikkelimanganaasikobolttiakkuihin (NMC).

Kaikissa kokeissa käytettiin bakteerien tuottamaa rikkihappoa ja onnistuneet liuotukset havaittiin pH:n ja hapettumis- ja pelkistymispotentiaalin (redox) muutoksina. Liuotuksen tehokkuusprosentit laskettiin induktiivisesti kytketyn plasmaoptisen emissiospektrometrin (ICP-OES) ja elektronimikroskoopin (SEM/EDS) tuloksista.

Epäsuora bioliuotus osoittautui tuloksien pohjalta potentiaaliseksi litiumioniakkujen kierrätystavaksi. Kokeissa käytettiin onnistuneesti korkeita massatiheyksiä ja lyhyttä reaktioaikaa. Litiumin ja manganaasin liuotukseen katalyytit eivät ole välttämättömiä, kuitenkin koboltin liuotuksessa niillä oli merkittävä vaikutus. Osa metalleista saostui korkeiden katalyyttikonsentraatioden takia. Katalyyttien yhtäaikainen käyttö osoittautui kannattamattomaksi, tähän liittyvien jatkotutkimuksien kannattavuus on syytä arvioida erikseen.

Tämä opinnäytetyö mahdollistaa jatkotutkimukset suuremmilla massatiheyksillä, erilaisilla akkutyypeillä tai esimerkiksi ultraäänen lisäämisen liuotuksen tehostamiseksi. Näissä tutkimuksissa tulisi käyttää suurempia näytemääriä parantamaan tulosten luotettavuutta.

Asiasanat:

bioliuotus, kierrätys, litiumioniakku, epäsuora liuotus, redox, NMC.

Content

Appendices

Figures

Pictures

Tables

List of abbreviations

CRM	Critical raw material
EDX	Elemental analysis system
EV	Electric vehicle
HL	High load lithium-ion battery
ICP-OES	Inductively coupled plasma optical emission spectrometry
IOB	Iron oxidizing bacteria
LFP	Lithium iron phosphate
LIB	Lithium-ion battery
NMC	Nickel manganese cobalt oxide
PSP	Portable handheld game console
PVDF	Polyvinylidene fluoride
SEM	Scanning electron microscopy
SOB	Sulphur oxidizing bacteria
SRM	Strategic raw material

1 Introduction

Scarce amount of natural resources nowadays and in the future, European Councils (2023) new regulation on batteries, and their recycling rates sets high incentive to the recycling of lithium-ion batteries (LIBs). Lithium recovery rate is set to be 50 % till the end of 2027 and 80 % by the end of 2031 (European Council 2023.) Lithium-ion battery pack prices decreased notably between 2010 and 2021, although forecasts for future prices have increased in recent years due to market disruptions (Carlier 2023, 24.) Future demand for metals used in battery production (Figure 1) also supports the price increase forecast.

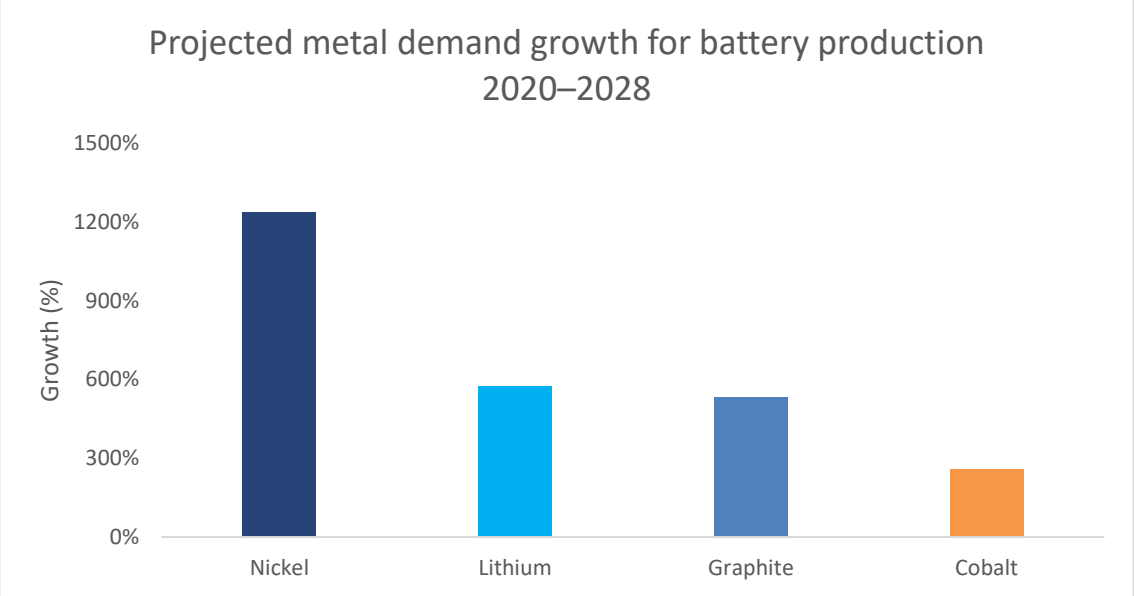

Figure 1. Metal demand increase from 2020 to 2028 (Mining Association Canada 2021).

Critical Raw Materials (CRMs) are a group of raw materials that are of both economic and strategic importance for the European economy but their supply carries a high level of risk. These materials are used in a variety of industries such as environmental technologies, consumer electronics, health, steel-making, defence, space exploration, and aviation. Not only are they crucial for the sustainable functioning of the European economy, but they are also critical for future applications and key industry sectors as there are no substitutes due to their unique properties. (CRM Alliance n.d.).

European Commission (2023) published its 5th list of CRMs as part of critical raw materials act, including a new addition of Strategic Raw Materials (SRM), which are materials used in strategic sectors e.g., defence and space technologies. Most notable

additions related to LIBs are copper, manganese, and nickel, whilst lithium, aluminium and cobalt kept their position in the CRM list. (CRM Alliance n.d., European Commission 2023, 4.)

Electrical vehicle market revenue has increased 10 fold in the past 8 years, and is estimated to double from the current state by 2028 reaching to 900 billion USD as shown in Figure 2.

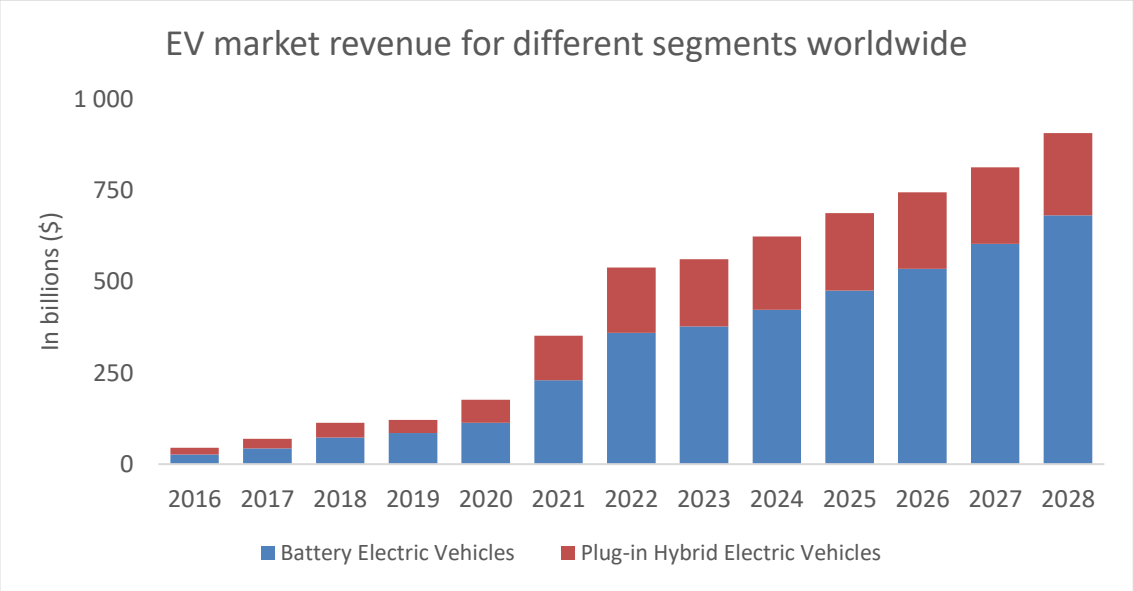

Figure 2. EV market revenue worldwide (Statista market insights 2023.)

1.1 Lithium-ion batteries

Lithium-ion batteries are widely used in many of our everyday devices e.g., laptops, mobile phones, cameras, watches and EVs due to the their higher cell voltage and energy density, as well as their longer lifespan (Dobó et al. 2023, 6363).

Anode, cathode, separator, and electrolyte are the four main components of LIBs. Negative electrode (Anode) is commonly carbon based e.g., carbon graffite, which holds lithium in its layers. Polyvinylidene fluoride (PVDF) binder is attached to carbons active material. Cathode is a mixture of carbon powder, Li-oxides, e.g., $LiCoO_2$ (LCO), $LiFePO_4$ (LFP) or $LiNi_xCo_yMn_zO_2$ (NMC), PVDF binder and aluminium foil, which covers the Li-oxides. Separator is usually made out of polypropylene (PP) or polyethylene (PE), and is located between cathode and anode to prevent the direct contact of electrodes, and short circuiting. Electrolytes allow ions to transfer from cathode to anode and vice

versa, salt solution that contains lithium e.g., $LiClO_4$ is dissolved in organic solvent. (Dobó et al. 2023, 6389.)

1.2 Recycling methods

There are four main ways to recycle LIBs; (i) direct recycling, (ii) pyrometallurgy, (iii) hydrometallurgy and (iv) biohydrometallurgy (bioleaching), though pretreatment is needed for most of the methods. Sorting, discharge, dismantling, mechanical-, solvent-, and thermal pretreatments are commonly used. Pretreatment is done to disintegrate the complex structure of the batteries for furter downstream processes. Pretreatment enhances metal recovery rate, decreases consumption of energy, and provides reduction to environmental risks. (Makwarimba et al. 2022, 6; Biswal & Balasubramanian 2023, 5–6.)

LIBs can be sorted according to their size, shape, density, magnetic properties and cathode chemistry. Batteries are often discharged in order to avoid unwanted explosion with brine/electrolyte methods, where a salt solution (NaCl or Na_2SO_4) is applied. Cryogenic- and electrical discharging can also be used along with thermal deactivation. Disassembling can be done either automatically or manually to separate different LIB components for further processing. (Biswal & Balasubramanian 2023, 6.) Pre-treatment methods are shown below in Figure 3.

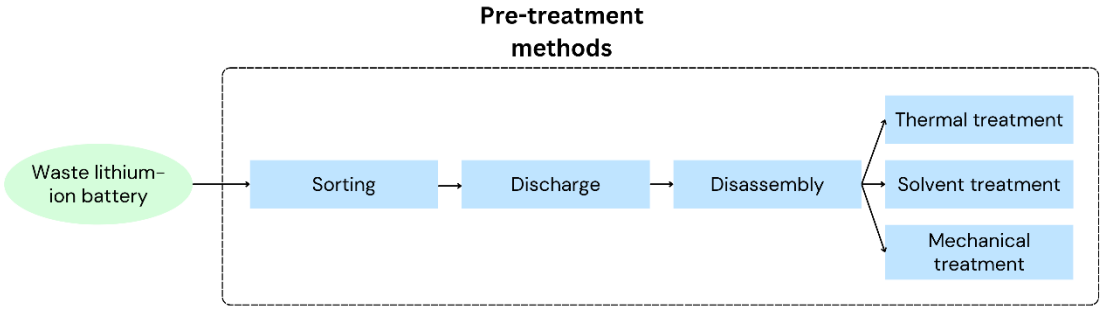

Figure 3. Schematic of pre-treatment methods.

In mechanical pre-treatment LIBs are grinded physically to one powder that contain both cathode and anode. They can be separated due to their different characteristics, by e.g., magnetic separation (Bae & Kim 2021, 3239).

Different solvents are used to separate active material from Al and Cu foils, the additive binder material is removed. Calcination is the final technique used to separate

carbon and organic material from LIB by using temperatures between 150–500 °C. PVDF binder can also be removed by using temperatures between 250–350 °C. (Bae & Kim 2021, 3239).

Direct recycling

Direct recycling aims to recover active materials from LIBs while preserving their compound structure, with less hazardous emissions and waste than other methods. Active materials are recovered with pre-treatment steps of discharging, dismantling, and separation of battery sections. (Chen et al. 2019, 2635–2637; Dobó et al. 2023, 6385; Biswal & Balasubramanian 2023, 8.)

Solid-phase sintering is a simple Li regeneration process using solid-phase Li agents to replace lost Li, requiring high temperatures. Hydrothermal re-lithiation involves treating spent battery material with an excess Li source solution, allowing lithium to incorporate into spent cathodes. (Chen et al. 2019, 2637; Dobó et al. 2023,6385–6387.)

However, all methods are primarily at the lab scale due to a variety of cathode chemistries and low recovery rates. Direct recycling could be viable for LFP recycling, as other methods aren't considered due to LFPs value. (Chen et al. 2019, 2635–2637; Dobó et al. 2023, 6385–6387; Biswal & Balasubramanian 2023, 8.)

Pyrometallurgy

Pyrometallurgy, a thermal processing method conducted at high temperatures ranging from 500 to 1,000 °C, serves to convert metal-containing components of batteries into metallic alloys. This technique is widely adopted due to its speed, operational simplicity, and adaptability. Furthermore, pyrometallurgy eliminates the need for battery pre-sorting. It involves a series of steps including pre-heating, combustion of plastic components, and reduction of metals. Various thermal treatments such as incineration, calcination, and pyrolysis are employed for cathode material recovery, followed by roasting or smelting processes for metal enrichment. The efficiency of pyrometallurgy hinges upon factors such as processing temperature, duration, flux composition, and purge gas type. Despite its industrial viability for large-scale lithium-ion battery (LIB) recycling, pyrometallurgy demonstrates limited effectiveness in lithium recovery. (Chen et al. 2019, 2627–2629; Dobó et al. 2023, 6372–6374; Biswal & Balasubramanian 2023, 7.)

Smelting emerges as a particularly efficient option for extracting valuable elements from spent LIBs, owing to its productivity and simplicity. During smelting, LIB components are heated to melt metallic elements, yielding metal alloys and slag fractions. Metal alloys containing valuable elements like Ni, Co, and Cu can be further processed through hydrometallurgy, while the slag fraction, containing lithium and manganese, may undergo hydrometallurgical treatment or be repurposed in the cement industry. (Dobó et al. 2023, 6372.)

Another pyrometallurgical approach for LIB recycling involves thermal reduction, wherein cathode materials are heated with a reducing agent like coke or charcoal to yield intermediate compounds suitable for subsequent refinement. Notably, waste anodic graphite material proves to be an effective and economical reductant in this process, offering high metal recovery rates and lower energy consumption compared to high-temperature smelting. (Dobó et al. 2023, 6373.)

Dobó et al. (2023, 6374) describe salt-assisted roasting, as a method that aims to convert metallic compounds into water-soluble salts by roasting with specific salts, thereby enhancing recycling effectiveness, reducing hazardous emissions, and lowering acid consumption. This technique, encompassing nitration, chlorination roasting, and sulfation roasting, leverages salts characterized by volatility, solubility, and low melting points.

Pyrometallurgical processes are prevalent in industry due to their simplicity and productivity. Advantages include the maturity of the process, obviating the need for sorting and size reduction, and yielding elemental components suitable for synthesizing various cathode materials. However, challenges such as CO_2 emissions and high energy consumption during smelting, the need for further processing of alloys, incomplete recovery of LIB materials, and potential inadequacy for electric vehicle (EV) batteries as the industry is shifting away from the use of cobalt. (Chen et al. 2019, 2627.)

Hydrometallurgy

Hydrometallurgy is employed to recover high-value elements from LIBs e.g., manganese, lithium, nickel, and cobalt after pre-treatment. It involves two phases, leaching, and recovering CRMs from leachate (Dobó et al. 2023, 6378). LIBs are leached in acids or bases, and separation can be done with various techniques e.g., ion-, solvent extraction, chemical precipitation, and electrolysis (Chen et al. 2019, 2630).

Chen et al. (2019, 2630–2633), Biswal & Balasubramanian (2023, 7–8), and Dobó et al. (2023, 6378–6381) agree that hydrometallurgy can yield high material purity, most CRMs can be recovered, low operation temperature can be achieved, and better environmental suitability compared to pyrometallurgical methods. However the pre-treatment requirement increases the cost and complexity of the recycling process, and some metals offer challenges in their separation. Disposal of the produced wastewater can bring additional costs.

Dobó et al. (2023, 6379) categorize LIB leaching into three methods; alkali leaching, acid leaching, and bioleaching.

The interaction between metallic elements and hydroxide ions in alkali solution is called alkali leaching. Typically, NaOH serves as the alkaline agent for leaching battery materials, selectively extracting aluminum due to its solubility in both alkali and acidic environments. At the same time, metals such as manganese, cobalt, and nickel remain insoluble in alkali solutions. Ammonia is also used, because of its ability to form stable ammonia complexes with metals, e.g., Ni, Co, and Cu. The process is also selective, with the possibility of avoiding expensive separation or purification steps, explaining the recent growing interest in the method. (Chen et al. 2019, 2631; Dobó et al. 2023, 6381.)

Acid leaching is divided into inorganic- and organic acid leaching, while inorganic acids techniques are prevalent due to high recovery efficiency, they produce hazardous gas emissions and waste acids. Commonly used inorganic acids are HCl, H_2SO_4, and HNO_3. Organic acids are more environmentally friendly while offering similar leaching efficiency, they consist of citric acid, ascorbic acid, oxalic acid, and formic acid. (Chen et al. 2019, 2631; Dobó et al. 2023, 6379–6381.)

Acid leaching is often combined with the addition of a reducing agent usually H_2O_2 to convert the less soluble metal such as Co^{3+} or Ni^{3+}, to their more soluble state Co^{2+} or Ni^{2+} (Harper et al. 2019, 81). Na_2SO_3 can also be used to improve the efficiency of the leaching process (Chen et al. 2019, 2631; Dobó et al. 2023, 6379).

Biohydrometallurgy

Bioleaching has risen in popularity in recent years, due to the process producing less emissions, being cost-effective, and requiring less energy, whilst maintaining high efficiency. (Chen et al. 2019, 6381; Biswal & Balasubramanian 2023, 8–9; Dobó et al. 2023, 2630.)

In bioleaching, microorganisms (bacteria or fungi) generate organic- or inorganic acids to leach the LIBs, it has been proven to be a viable method in the mining industry (Harper et al. 2019. 83). The biggest drawbacks are the possibility of contamination and long cultivation times (Biswal & Balasubramanian 2023, 9). Fungi have better toxic tolerance compared to bacteria, therefore it is more often used to recover heavy metals from solid refuse states Dobó et al. (2023, 6381).

The bacteria commonly used in bioleaching are acidophilic sulphur-oxidizing (SOB) and iron-oxidizing bacteria (IOB). *Acidithiobacillus thiooxidans, Sulfobacillus thermosulfidooxidans* and *Alycyclobacillus* spp*.* are the most common SOBs, while IOBs are *Acidithiobacillus ferrooxidans* and *Sulfobacillus* spp. They obtain carbon by reductive fixation of atmospheric CO_2 which acts as their carbon source, while energy source for IOBs is ferrous ion (Fe^{2+}) and sulphur (S^0) for SOBs. (Biswal & Balasubramanian 2023, 9–10.) Carbon fixation, sulphur- and iron oxidation are shown below in equations 1–3.

$$S^0 + O_2 + 2\,H_2O \xrightarrow{SOB} 2\,H^+ + SO_4^{2-}, \quad (1)$$

$$4\,Fe^{2+} + 4\,H^+ + O_2 \xrightarrow{IOB} 4\,Fe^{3+} + 2\,H_2O, \quad (2)$$

$$6\,Co_2 + 12\,NADPH_2 + 18\,ATP \xrightarrow{SOB\ \&\ IOB} C_6H_{12}O_6 + 12\,NADP + 18\,ADP + 18\,Pi, \quad (3)$$

Aspergillus niger is a fungus that is often used in bioleaching, it breaks down metal-containing compounds into basic elements, which gives it the required energy to secrete biological acids, e.g., citric, oxalic, and gluconic acids. (Li et al. 2023, 2.)

Bioleaching is divided into two main methods, contact-and non-contact leaching. Both methods utilize the metabolism of fungi and bacteria. Contact leaching is further divided into one-step and two-step leaching. (Biswal & Balasubramanian 2023, 9; Li et al. 2023, 3.)

One-step method is optimal for less toxic LIBs, where the pregrown bacteria are inoculated to the leaching media containing LIB black mass (BM). In this method the bacteria keep growing and producing acids whilst leaching the metals. However this methods requires more pre-processing steps as the bacteria are susceptible to decreased growth rate due to the toxicity of the LIBs and the alkalinity of the material. (Biswal & Balasubramanian 2023, 9; Tezyapar Kara et al. 2023, 3337; Li et al. 2023, 3–7.)

Biswal & Balasubramanian (2023, 9) explain that two-step method is better suitable for toxic materials and requires less pre-processing as the microorganisms are first grown to e.g., logarithmic phase for the acid production (step one), before addition of BM (step 2).

The preferred method as it produces highest leaching efficiency is non-contact or spent medium leaching as the bacteria or fungi produce the desired acids and the cells are later removed by centrifugation or filtration or combination of them. This method allows us to investigate the effects of different pulp densities as no apoptosis is present. (Biswal & Balasubramanian 2023, 9.)

1.3 Factors influencing bioleaching

Bosecker (1997, 595–596), Roy et al. (2021, 8), Biswal & Balasubramanian et al. (2023, 15) and Li et al. (2023, 7) all agree that major influncing factors for bioleaching are, type of microorganisms or their mixtures (bacteria and fungi), pH of the leaching solution, amount of nutrients, temperature, aeration, catalysts, and LIBs pulp density.

The leaching medium pH is kept at pH range of 1 – 4 with IOBs and SOBs for optimal growth, whilst fungi have higher pH range between 3 – 7. Most of IOBs and SOBs optimal temperature is 28 – 30 °C, (Bosecker 1997, 595; Roy et al. 2021, 8; Biswal & Balasubramanian 2023, 16). Acid concentration has a major effect on improving leaching efficiency (He et al. 2017, 174–175).

In bacterial leaching with IOBs that use Fe^{2+} (e.g., $FeSO_4 \times 7\ H_2O$) as energy source, waste iron scrap can be used to reduce recycling, and overall process costs. Pyrite can act as a energy source for SOBs, while fungi can utilize organic carbon containing waste. (Roy et al. 2021, 8; Biswal & Balasubramanian 2023, 15–16.)

Boysecker (1997, 595.) and Roy et al. (2021, 8.) points out the importance of sufficient oxygen supply by aeration, stirring or shaking to growth optimization of microorganisms, whilst CO_2 is needed with certain organisms.

Generally studies have pulp densities between 1 to 5 % (w/v) (Tezyapar Kara et al. 2023, 3340.) It plays major role in bioleaching due to the metal toxicity and its effect on microorganisms survival (Bosecker 1997, 595–596). Microorganisms can also be adapted for the better survival against toxicity. (Roy et al. 2021, 8; Li et al. 2023, 4–5.)

Biswal & Balasubramanian (2023, 17–18) and Li et al. (2023, 7–9) explain the importance of external catalysts to enhance the process speed, and efficiency. Vieceli et al. (2023, 9663) inform that addition of reducing agents (e.g., H_2O_2, Fe^{2+}) is to reduce

transition metals to reach lower, thus more leachable valence states (e.g., Co^{3+} to Co^{2+}), which is also supported by Jha et al. (2013, 1892) and Ghassa (2020, 1–2; 2021, 1–2). Different metallic ions can also be used e.g., Ag^{+}, Cu^{2+} and Co^{2+}. Biswal & Balasubramanian (2023, 17–18) add ultrasonication as a recent method to enhance leaching efficiency.

1.4 Metal recovery

Dobó et al. (2023, 6381–6382) and Chen et al. (2019, 2633–2634) concur that solvent extraction, chemical precipitation, electrolysis and ion-exchange are all viable methods for metal separation or impurity removal.

Solvent extraction is an effective and commonly used approach to separate metals, it uses the solubility variations of metal ions in solvent versus aquaeous liquid. As a process it is fast, and provides high purity yields, although solvents are expensive and the process itself is complex. (Chen et al. 2019, 2633; Dobó et al. 2023, 6381–6382.)

Chemical precipitation is a commonly used way due to its ability to remove impurities, and precipitate valuable metals through change of pH and temperature. CO_3^{2-} containing salts e.g., $(NH_4)_2CO_3$ are frequently used as precipitants. Due to Ni, Mn and Co sharing similar properties, they have been coprecipitated together and sintered the precursor into cathode material of NMC. (Chen et al. 2019, 2633–2634; Dobó et al. 2023, 6382–6383.)

Chen et al. (2019, 2634) and Dobó et al. (2023, 6383) acknowledge sol-gel synthesis as a way to synthesize cathode material by adjusting the ratio of metal ions. After adjusting, metal ions are distributed in sol states. Mixture of precursors are then hydrolyzed for the sol to transform into gel state. Finally gel is heated to produce the solid products.

Electrowinning is a commonly used electrochemical method for metal extraction, it uses the electrolytic solution where metals are dissolved in. Basic electrowinning unit comprises of a tank, rectifier and a pump. Electrolytic solution is transferred to tank with the pump, while cathodes and anodes are inside the tank. Electrowinning rectifier provides electrical current to both cathodes and anodes, causing the cations to move toward cathode due to electrical potential differences. (Barshai 2016.) Vegliò et al. (2003, 246–252) used electrowinning to successfully extract nickel and copper with great efficiency after sulphuric acid leaching of electric waste. Lister et al. (2014, 229) inform that the metals reduction potential needs to be similar and that mixed metal

solution can complicate the process as noble metals could prevent the polarization of metals that are less noble.

Ion exchange and electrodialysis are mentioned by Dobó et al. (2023, 6383) as recovery methods, but discarded as they are not commercial used due to their complicated operation and high costs.

Aim of the thesis was to investigate the viability of non-contact bioleaching for valuable metal recycling from spent lithium-ion batteries with different BM pulp densities as there were only limited studies available with high pulp densities as most studies are conducted with pulp densities between 1 to 5 % (w/v) (Tezyapar Kara et al. 2023, 3340.) Additionally, due to excellent results presented with the use of catalyst by Jha et al. (2013, 1892–1894), Xin et al. (2016, 255) and Ghassa (2021, 3–8) the effect of different catalysts with different concentrations were tested, especially the combined use of H_2O_2 and Fe^{2+} as only limited studies were available. Thesis was done at University of Natural Resources and Life Sciences - IFA-Tulln in Department of Agrobiotechnology, and it was part of FuLIBatter-project.

2 Materials and Methods

This chapter explains the theory behind the used analytical methods and contains the list of used materials.

2.1 Chemicals and equipment

All chemicals that were used in experiments were of analytical grade unless stated otherwise, and all dilutions were done with ultrapure water from Merk KGaA. Below in tables 1 and 3 are listed all used materials and equipment.

Table 1. List of used chemicals.

Material	Lot	Manufacturer
Biogenic acid (H_2SO_4)		Klemens Kremser et.al.
Hydrogen peroxide (H_2O_2)		
Iron sulphate heptahydrate ($FeSO_4$ x 7 H_2O)	10215738	Alfa Aesar (Thermo Fisher Scientific)
Natrium hydroxide (NaOH)		
Nitric acid (HNO_3)		

Table 2. Metal content in batteries.

	Metal content g/kg						
Battery	Li	Co	Ni	Mn	Cu	Al	Fe
NMC	27.60	145.0	58.60	41.70	35.50	52.60	5.75
LFP	24.6	0.88	3.52	1.21	58.4	16.9	177.0
HL	43.7	292.0	58.4	40.6	65.7	50.9	4.37
PSP	33.8	82.1	106.0	84.2	44.9	34.4	15.4

Above in Table 2 are the metal contents of each battery type. NMC has nickel manganese cobalt oxides as cathode material, while LFP has lithium iron phosphate. HL are LIBs collected from mobile phones and laptops and PSP are LIBs from powerbanks and electric bikes.

Table 3. List of used instruments.

Instrument	Model name	Manufacturer
Centrifuge	5427 R	Eppendorf
Incubator	Multitron Pro	Infors HT
pH-meter	S220	Mettler Toledo
pH electrode	LE422	Mettler Toledo
ORP electrode (Ag/AgCl)	InLab Redox	Mettler Toledo
Analytical scale/balance	MSE1203S-100-DE	Sartorius lab instruments
Scanning electron microscope	3030	Hitachi
Inductively coupled plasma optical emission spectrometer with SPS4 autosampler	5110	Agilent Technologies
Magnetic stirrer	Variomag Poly 15	Thermo Scientific

To determine active hydrogen ion concentration in aqueous solution pH scale is used. Acidic pH < 7, neutral pH = 7, alkaline pH > 7 (Ionode n.d.).

pH is defined as minus logarithm of H_3O^+ ion activity by Sørenson (Mettler Toledo 2023, 71–72):

$$pH = -\log([a_{H^+}]), \tag{4}$$

As shown in equation above, when pH value changes by one unit, H_3O^+ ion activity change is tenfold (Mettlero Toledo 2023, 71).

Mettler Toledo (2023, 71) reminds that pH theory is often explained with H^+ ions concentration with pH, while it should be referred to H_3O^+ ions.

$$H^+ + H_2O \leftrightarrow H_3O^+, \quad (5)$$

Oxidation-reduction potential (ORP or Redox) is a chemical substances tendency to oxidize or reduce another substance, expressed in millivolts (mV). After oxidization of a substance, its oxidation state increases. Adjacent oxidation states of a certain substance are referred as redox couples. E.g., Redox couple Fe^{2+}/Fe (Emerson 2008, 1).

$$Fe = Fe^{2+} + 2e^-, \quad (6)$$

Where,

Fe is iron,
Fe^{2+} is ferrous ions,
$2e^-$ are electrons.

Above shown reaction is half-reaction, as the remaining electrons need to be taken by another substance, therefore another substance is needed (Emerson, 1).

Ideal ORP follows the Nernst equation (Ionode n.d.):

$$E_{eq} = E^0 + \left(\frac{RT}{nF}\right) * \ln\left(\frac{Ox}{Red}\right), \quad (7)$$

Where

E_{eq} is ,
R is universal ideal gas constant,
T is temperature in kelvins,
n is the number of electrons transferred,
F is the Faraday constant,
E^0 is standard electrode potential,
Ox is concentration of oxidized species e.g., Fe^{3+},
Red is concentration of reduced from of redox couple Fe^{2+}.

ORP measurement principle is the use of an inert metal electrode, e.g., platinium or gold, they are able to either receive or release electrons due to their low resistance. ORP measurement will continue until it reaches potential, due to charge build up, being equal to solutions ORP. (Emerson 2008, 1–2.)

2.2 Inductively coupled plasma optical emission spectroscopy

Inductively Coupled Plasma Optical Emission Spectroscopy (ICP-OES) is an analytical technique for determining the amount of a specific element is in a sample (Agilent 2023). It is commonly used applications e.g., trace element analysis in human brain, pesticide screening and determining the purity of pharmaceutical compounds, due to its ability to analyze complex samples. Drinking water, wine, and petrochemicals have also provided regular use for the technique. (Levine 2023.)

High-energy plasma is generated by introducing a spark generated by radio frequency or microwave irritation directed to metal coils to ignite argon gas, which flows to two glass glass tubes, last tube is used for the aerosolized sample carried with argon. (Agilent 2023; Levine 2023.)

To analyze a sample with this plasma, the sample needs to be aerosolized and transported to the point of interaction with the plasma matrix. This is usually done through a nebulizer. When the plasma interacts with the sample, it degrades the sample into individual elements, each of which has a characteristic optical signal that can be detected spectroscopically. (Levine 2023.)

Sometimes interpreting results can be tricky due to multiple elemental signal overlapping. To detect each element separately, wavelengths are separated with an optical grating device. The final sample composition is determined by a detector and signal processor after light wavelengths have been correlated to specific element identities. Before measurements, the detector is calibrated with known concentrations of elements that are measured for effective quantitation. Signals that can potentially compromise the analyte detection have to be removed at the end. (Levine 2023.)

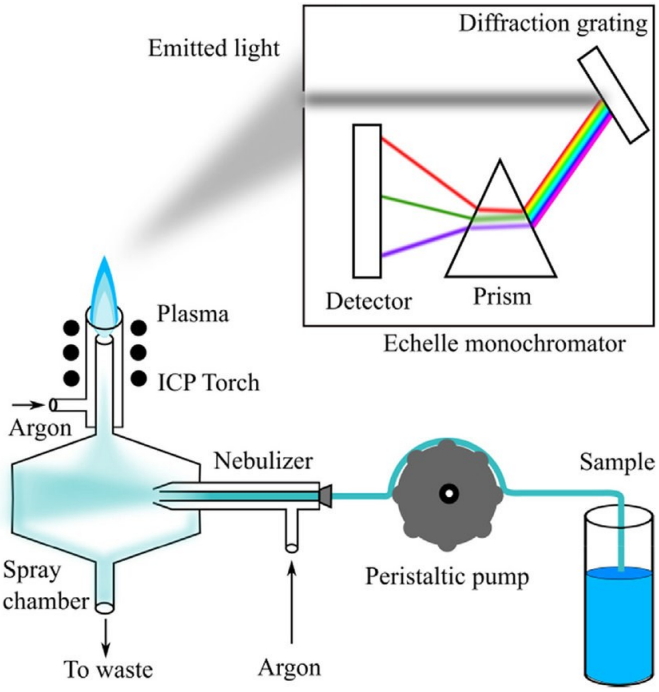

Picture 1. ICP-OES working principle (Cherevko & Mayrhofer 2017, 328).

General working principle of ICP-OES, and the common parts are illustrated in Picture 1. Sample preparation protocol is described in detail in Appendix 2.

2.3 Scanning electron microscopy with energy dispersive X-ray spectroscopy

A scanning electron microscope (SEM) is a widely used technique in various fields of science and engineering. Common applications are in materials-, biological-, geological- and medical sciences. (O'Driscoll 2023.)

It creates a magnified image of a sample by projecting a focused beam of electrons into a sample. The beam is scanned across the surface of the sample. The electrons

that come out of the sample are used to create a magnified image. (Microscopy Australia n.d..) Components of an SEM are shown in Picture 2 below.

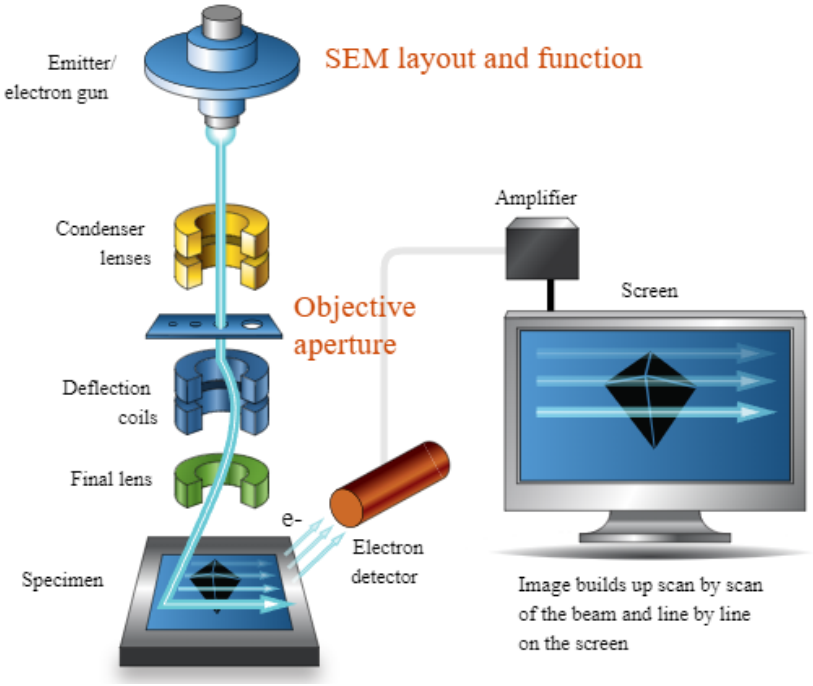

Picture 2. SEM components (Microscopy Australia n.d.).

Energy Dispersive Spectroscopy (EDS) also referred as energy dispersive X-ray spectroscopy (EDX) is an X-ray microanalytical technique, that can provide chemical composition information of samples, results can be either qualitative or quantitative. (Microscopy Australia n.d.).

X-rays that result from the interaction of an electron beam and sample can be background X-rays or Characteristic X-rays. Energy Dispersive detector displays the signal that it creates from X-rays as a spectrum, or histogram, of intensity versus Energy. Energies of X-rays allow the sample elements to be identified, whilst intensities of X-rays allow the concentration quantification. (Microscopy Australia n.d..)

2.4 Biogenic acid

All experiments used sulphuric acid that was produced with sulfur-oxidizing bacteria *A.thiooxidans* and moderately thermophile *A.caldus* in continuous stirred tank reactor in summer 2022 by Kremser et.al. (2022, 184).

To determine the concentration of the biogenic sulphuric acid (H_2SO_4), acid titration was performed with Bromethyl Blue as an indicator, sulphuric acid was diluted in 1:200 ratio for faster and successful titration. Data and results presented in Table 4.

Equilibrium equation, and calculation of H_2SO_4 concentration, results from the 1st titration used as an example.

Neutralization reaction of sulphuric acid with sodium hydroxide.

$$H_2SO_4 + 2NaOH \rightarrow Na_2SO_4 + 2H_2O, \quad (8)$$

Equations to calculate sulphuric acid concentration

$$M_A = \frac{\left(\frac{M_B}{2}\right) * V_B}{V_A} * DF, \quad (9)$$

$$c(H_2SO_4) = \frac{0{,}05\,\frac{mol}{l} * 5{,}3\ ml}{100\ ml} * 200 = 0{,}53\,\frac{mol}{l}, \quad (10)$$

Where

c is concentration in mol*l^{-1},
M_A is molarity of H_2SO_4 in mol*l^{-1} ,
M_B is molarity of NaOH in mol*l^{-1} ,
V_B is the used volume of NaOH,
V_A is the volume of H_2SO_4,
DF is dilution factor.

Table 4. Determining sulphuric acid concentration by acid titration

	1st	**2nd**
Concentration of NaOH (mol*l^{-1})	0,1	0,1
Initial volume of NaOH (ml)	18,9	13,6
Final volume of NaOH (ml)	13,6	7,5
Used volume of NaOH (ml)	5,3	6,1
Concentration of H_2SO_4 (mol*l^{-1})	5,3	6,1

3 Bioleaching

This chapter presents the experimental procedures for bioleaching experiments that were conducted for the thesis to determine the efficacy of biogenic sulphuric acid (H_2SO_4) for black mass leaching.

3.1 Bioleaching performance at different pulp densities

This section investigates the non-contact bioleaching of varying pulp densities on the bioleaching performance with two concentrations: 6 % and 10 % and battery types NMC, LFP, HL and PSP. Both experiments were executed in triplicates in 50 ml conical erlenmayer flasks with 50 ml of H_2SO_4 and stirring speed of 200 rpm at room temperature.

The first experiment was conducted to examine non-contact bioleaching with 6 % (w/v) pulp density of BM. Experimental time was set to 48 hours. Samples were taken at 1 hour intervals until 6 hours and at 24 and 48 hours. Fresh biogenic acid was added to replace the amount of sample taken excluding the last time point. Liquid samples were then filtrated through 0.45 µm nylon filter before pH measurements, and prepared for ICP-OES analysis according to sample preparation protocol received from IMC Krems, which is described in (Appendix 1).

At the end of the experiment, the remaining lixiviant was centrifuged at max speed for 25 minutes, and the supernatant was discarded. The remaining pellet was dried, weighed and measured with SEM/EDX as described later in chapter 4.1

Reduced leaching time to 2 hours in the second experiment with 10 % (w/v) pulp density. During the course of the experiment, 1 ml samples were taken in 20 minute intervals and fresh biogenic acid was added after samples were taken, excluding the last timepoint, pH and redox were measured after filtration. Samples were then prepared for ICP-OES analysis as explained earlier.

3.2 Application of different catalysts

Experiments to test the effect of Fe^{2+} and H_2O_2 separately and combined as catalysts were conducted with NMC as sole battery material, at room temperature, duration for the experiments were set to 2 hours each, 1 ml samples were taken at 20 minute intervals, shaking speed was kept at 200 rpm throughout the experiment, 5 g of NMC

powder was added to 50 ml of H_2SO_4. At the end of the experiment supernatant was filtered, and prepared for ICP-OES analysis as described in previous chapter.

Table 5. Input values for Modde.

Name	Abbreviation	Units	Type	Settings
Hydrogen peroxide	H_2O_2	%	Multilevel	1, 5, 10
Ferrous ion	Fe^{2+}	g/l	Multilevel	1,68; 3,35; 6,7

The first experiment tested the combined use of Fe^{2+} and H_2O_2, input parameters that are shown above in Table 5 were used to design the experiment with Modde software from Sartorius. Experimental setup that was used is shown in Table 6. Excess foam forming was observed with samples containing 10 % of hydrogen peroxide (N3, N6, N9-N11), therefore the experiment had to be repeated with these samples in larger 250 ml conical erlenmayer flasks to prevent foam formation.

Table 6. Design of experiment obtained from Modde.

Sample	Fe2+ (g/l)	H2O2 (%)
N1	1,68	1
N2	3,35	5
N3	6,67	10
N4	1,68	1
N5	3,35	5
N6	6,7	10
N7	1,68	1
N8	1,68	1
N9	6,7	10
N10	6,7	10
N11	6,7	10
N12	1,68	1
N13	1,68	1

To examine the difference in leaching efficiency with Fe^{2+} and H_2O_2 in the second experiment was executed in duplicates, catalyst concentrations are shown in Table 7 below.

Table 7. Experimental setup with a single catalyst.

Sample	Fe^{2+} (g/l)	H_2O_2 (%)
NF1-2	1,68	
NF3-4	3,35	
NF5-6	6,7	
NH1-2		1
NH3-4		5
NH5-6		10

4 Results and discussion

This chapter presents the results of the experiments executed for the thesis and the discussion is provided at the end of the chapter. Only NMC results are displayed for better comparability and to reduce the amount of figures.

Copper was removed from all results after Figure 5, as the NMC contains only small amounts of copper.

Leaching efficiency is calculated from ICP-OES results by dividing the amount of metal ions in leachate with the amount of metal ions in original sample, and multiplied with 100 to have the percentages (Sibananda & Niharbala 2023, 7195).

Formula to calculate leaching efficiency (Sibananda & Niharbala 2023, 7195).

$$Leaching\ efficiency\ (\%) = \frac{c(metal\ ions\ in\ leachate)}{c(metal\ ions\ in\ original\ sample)} \times 100, \qquad (11)$$

4.1 Bioleaching performance at different pulp densities

This section presents and analyses the results obtained with bioleaching of waste LIB cathode powder with pulp densities of 6 % and 10 % with battery types NMC, LFP, HL and PSP.

According to Xin et al. (2016, 251–252) and Ghassa et al. (2020, 2) acid dissolution by the biogenic acid is the sole mechanism for Li^+ release. Due to insoluble higher valence states of Co^{3+} , Mn^{4+} and Ni^{3+} they need to be converted into soluble lower valence states Co^{2+}, Mn^{3+}, Ni^{2+}. Leaching equations by Xin et al. (2016, 252) are shown below.

$$Li_2O + H^+ \rightarrow Li^+ + H_2O, \qquad (12)$$

$$X^{4+}"/"X^{3+}(X = Co, Mn, Ni) + e \rightarrow X^{2+}(XO), \qquad (13)$$

$$XO + H^+ \rightarrow X^{2+} + H_2O, \qquad (14)$$

where,

X is Co, Mn, Ni.

Black mass pulp density of 6 % (w/v)

Solubilization of metals and the consumption of sulphuric acid can be seen as pH change shown in Figure 4.

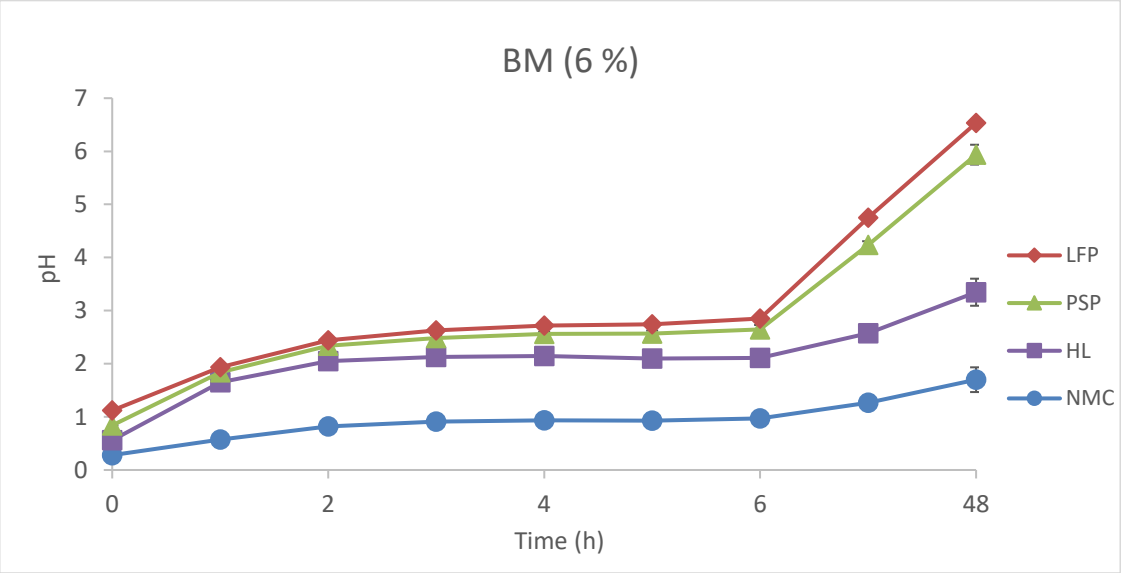

Figure 4. pH change in 48 hours, BM 6 %.

Normalized weight percentage of metals was measured from remaining dried BM samples, and the original samples with SEM/EDX as shown in Figure 5, results are to support the findings and results of ICP-OES results, as the sample size for EDX was too small for it being quantitative.

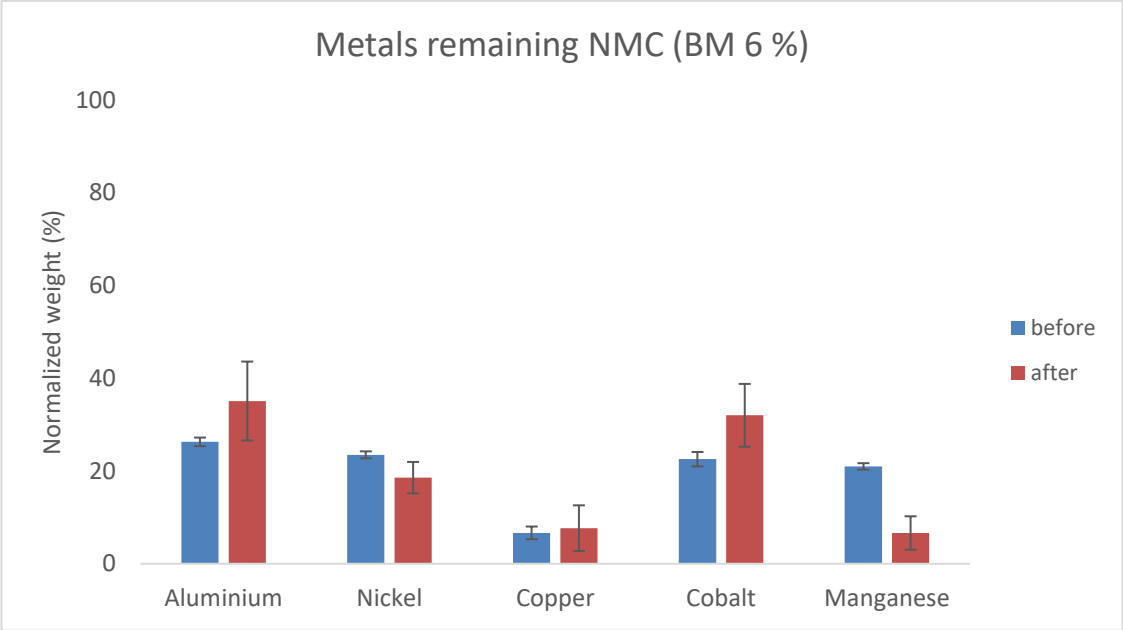

Figure 5. SEM/EDX results, before and after leaching.

After first hour of leaching all iron, lithium and manganese were leached, as well as over half of cobalt and aluminium as depicted in Figure 6. As the starting material and the samples were measured at different laboratories, it is likely that this caused the leaching efficiencies to exceed 100 %.

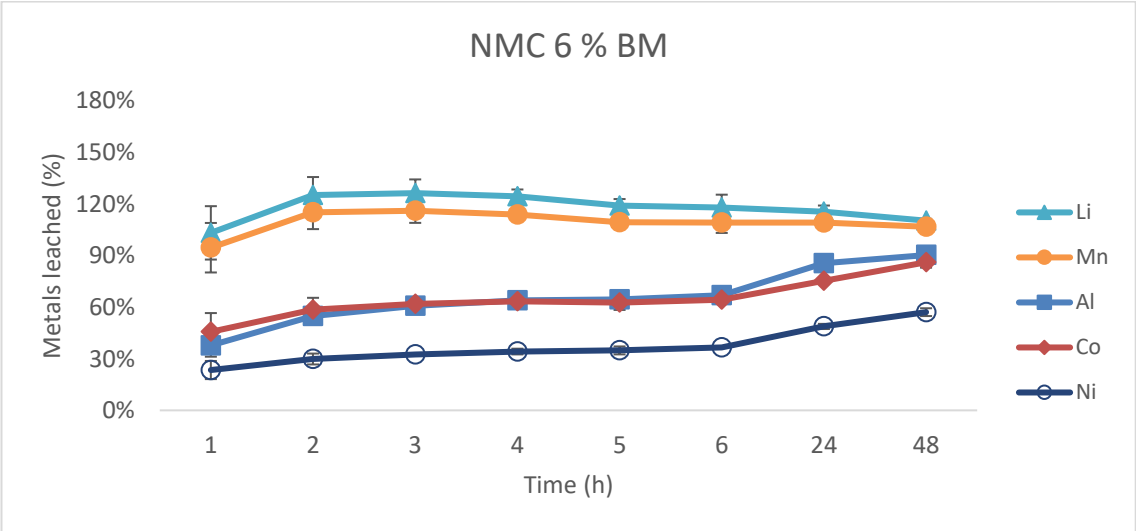

Figure 6. Leaching efficiency, 6 % BM.

Figure 7 displays the approximate amount of black mass leached, calculated by substracting the weight of remaining dried BM from the initial weight of BM in grams.

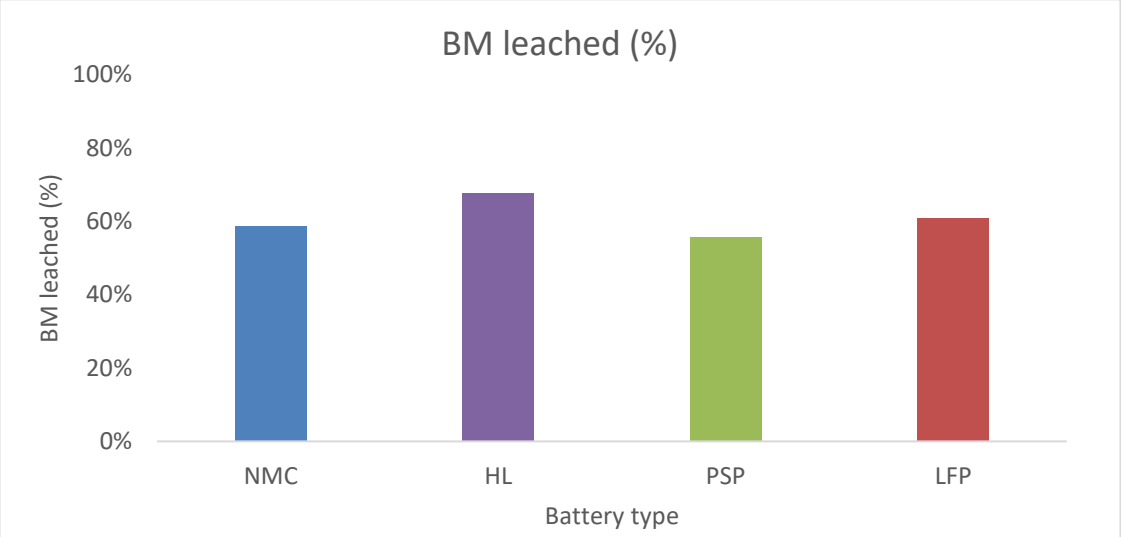

Figure 7. BM leached after 48 hours, pulp density 6 %.

High efficiency was reached after 2 hours as described earlier, and after pH increasing above 2 at 2 hours, leaching efficiency and pH change show only minor increase before 6 hours. Between 6 and 48 hours aluminium, cobalt, and nickel leaching efficiencies increased to (23.3 %, 22.8 %, 20.6 %).

Black mass pulp density of 10 % (w/v)

Pulp density was increased after excellent results from the experiment with 6 % (w/v) BM, leaching time was also reduced to 2 hours as there was only a minor increase in leaching efficiency after 2 hours.

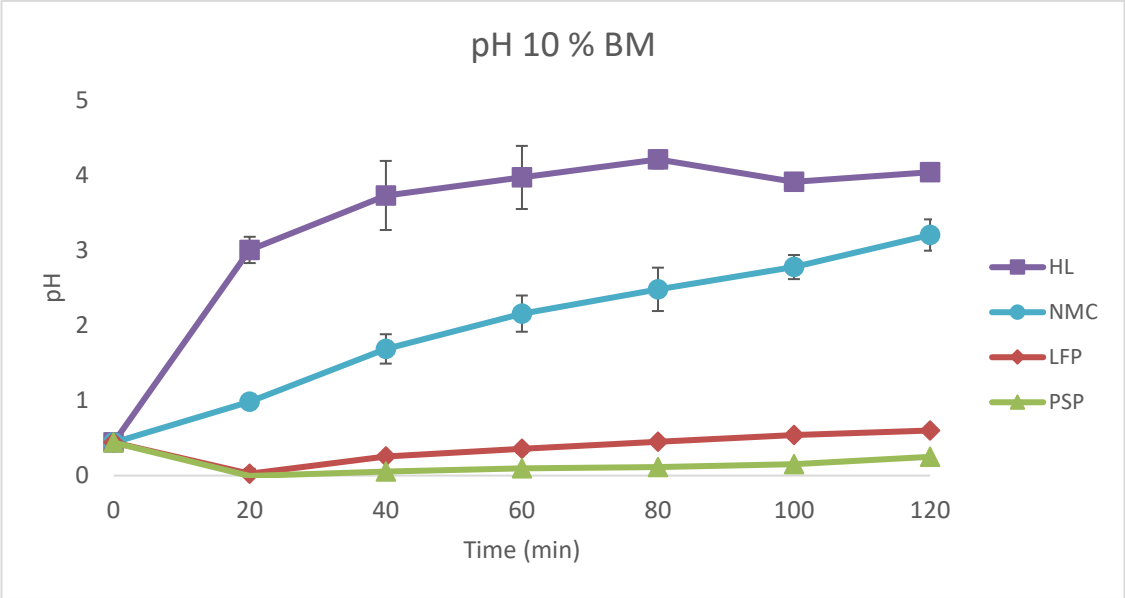

Figure 8. pH change in 2 hours of leaching with all battery types.

From Figure 8 we detect the fast pH increase in HL and NMC, whilst the pH of LFP and PSP first decreases, and then slowly increases over time.

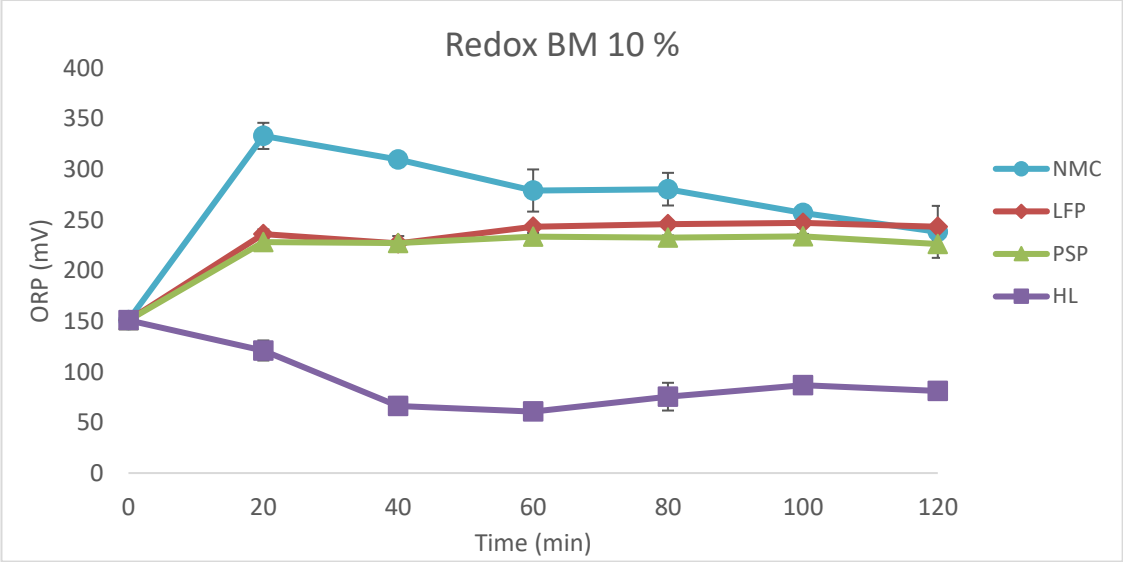

Figure 9. Redox potential after 2 hours of leaching with all battery types.

Redox potential shown in Figure 9 monitor the oxidation-reduction reactions, as leaching efficiency is increased with higher ORP values.

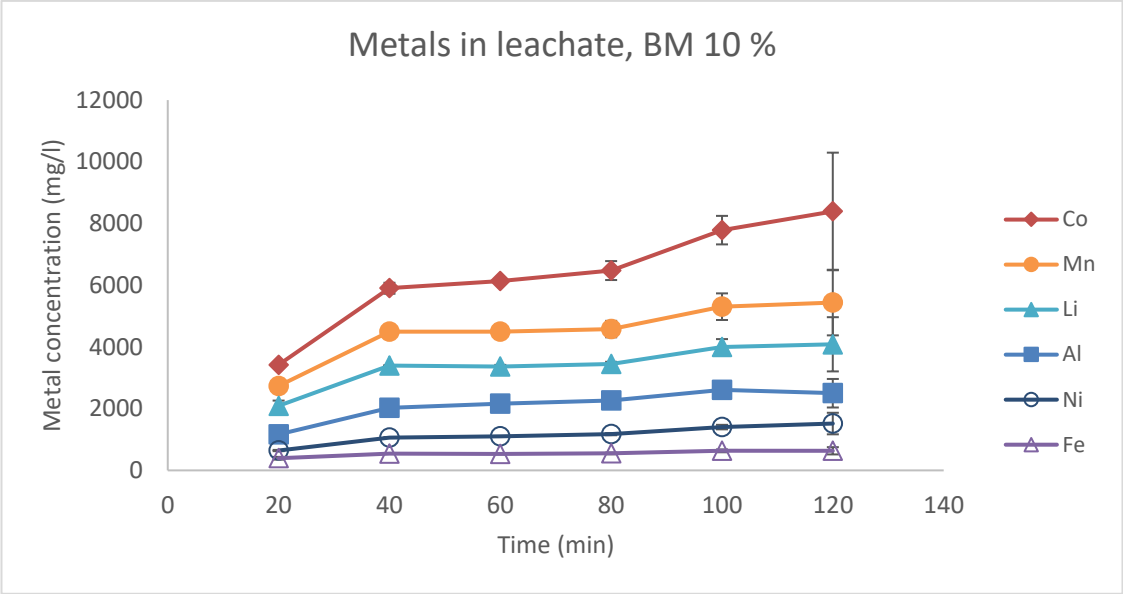

Figure 10. Leachate metal concentrations in mg/l with 10 % BM.

NMC samples containing BM with 10 % pulp density were measured with ICP-OES to obtain the metal concentrations in the leachate after 2 hours of leaching, results are shown in Figure 10.

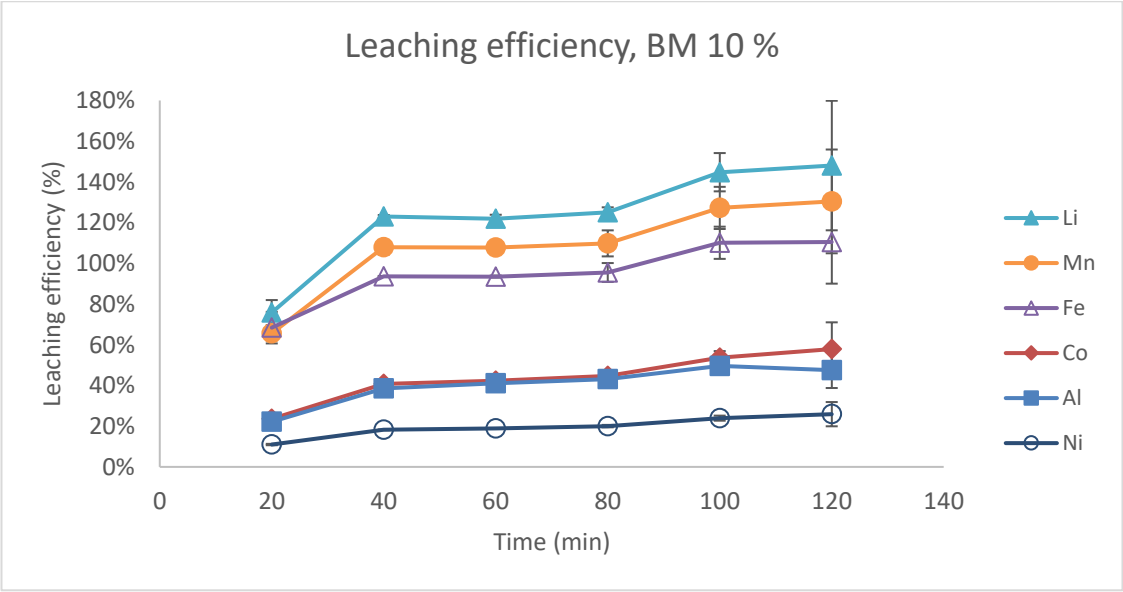

Figure 11. Leaching efficiency with 10 % BM.

ICP-OES results were compared to the original concentration of metals in BM to determine the leaching efficiency. Figure 11 display that 2 hour leaching time is

sufficient time for lithium and manganese leaching, as all of lithium 123.88 %, manganese 107.8 %, and almost all iron 93.6 % were leached after 40 minutes. After 2 hours following leaching efficiencies were achieved; cobalt 57.9 %, aluminium 47.5 % and nickel 25.9 %.

Leaching efficiency over 100 % is most likely caused by the experimental samples being measured in different laboratory than the initial BM analysis, and the possible difference between metal concentrations in grounded BM.

4.2 Bioleaching with applied catalysts

As explained by Jha et al. (2013, 1892) and Vieceli (2023, 9663), reducing agents are used to reduce the valence state of the metals to soluble one. Numerous studies have shown the efficacy of ferrous ions and hydrogen peroxide as reducing agents. Ferrous ions (Fe^{2+}) in studies by (Xin et al. 2016, 254–255; Ghassa et al. 2020, 1–2, 11–13; Ghassa et al. 2021, 2, 8) and hydrogen peroxide (H_2O_2) by (Jha et al. 2013, 1892–1893; Ghassa et al. 2020, 1–2; Ghassa 2021, 5–8; 507–510; Vieceli et al. 2023, 9664–9667). Equations for reduction reactions for cobolt are presented below with ferrous ions (Eq. 15) (Ghassa et al. 2021, 2) and hydrogen peroxide (eq. 16) (Jha et al. 2013, 1892).

$$2\mathrm{LiCoO_2} + Fe^{2+} + 3\mathrm{SO_4^{2-}} + 8H^+ \rightarrow Fe^{3+} + 2CoSO_4 + Li_2SO_4 + 4H_2\mathrm{O}, \quad (15)$$

$$2\mathrm{LiCoO_2} + 3H_2SO_4 + H_2O_2 \rightarrow 2CoSO_4 + Li_2SO_4 + 4H_2\mathrm{O} + O_2, \quad (16)$$

Iron was excluded from the results that used ferrous ions as a catalyst, as the iron concentrations of the samples were too high for accurate measurements.

Fe^{2+} or H_2O_2 as catalyst

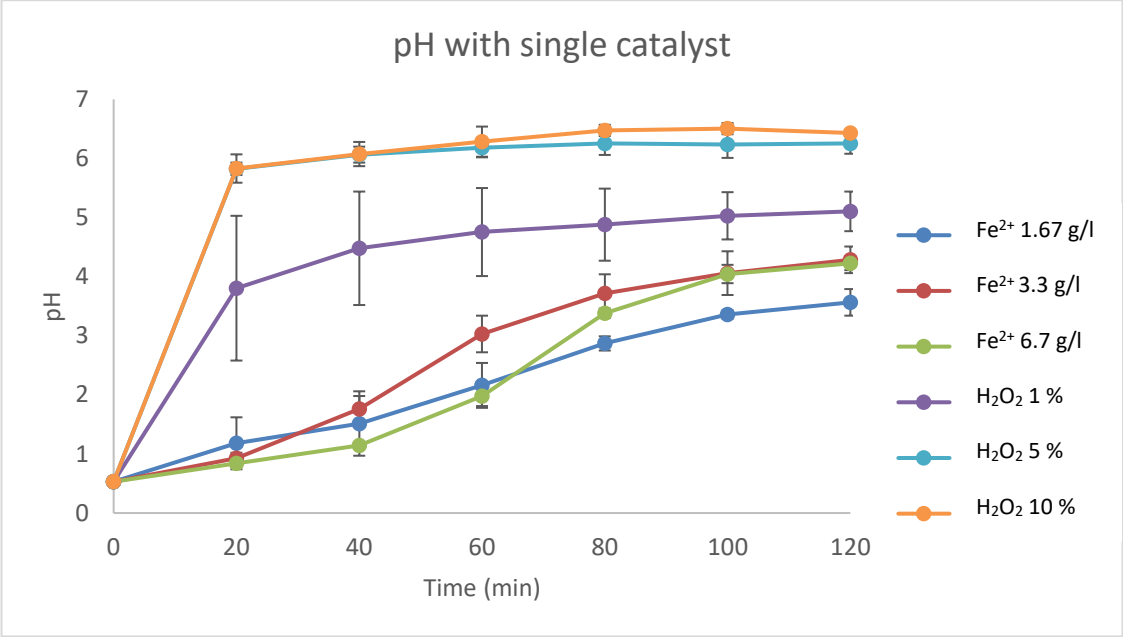

Figure 12. pH change with catalysts H_2O_2 or Fe2+.

When hydrogen peroxide is present in high concentrations of 5 % and 10 %, it causes an immediate increase in pH. Even with a lower concentration of 1 % hydrogen peroxide, the oxidization of metal ions in leachate is supported, as shown in Figure 12. This figure depicts the use of ferrous iron as a reducing agent, which appears to have a steadier effect on increasing pH.

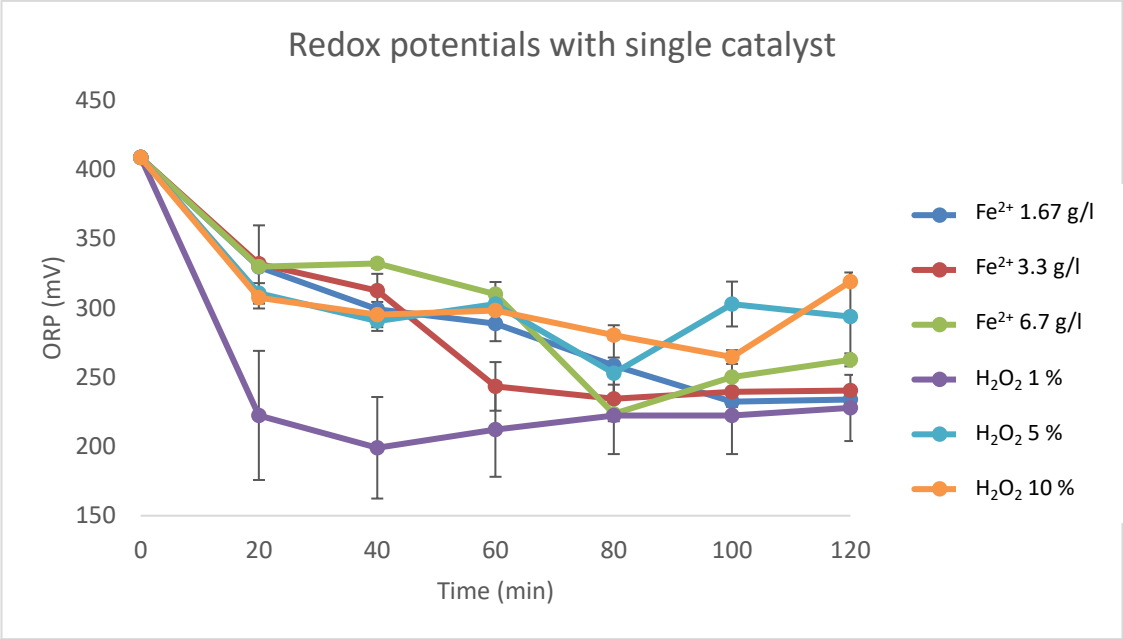

Figure 13. Redox change with catalysts H_2O_2 or Fe^{2+}.

Decrease in electron activity shown in Figure 13 indicates the change in oxidation- or reduction power, therefore metals being solubilized.

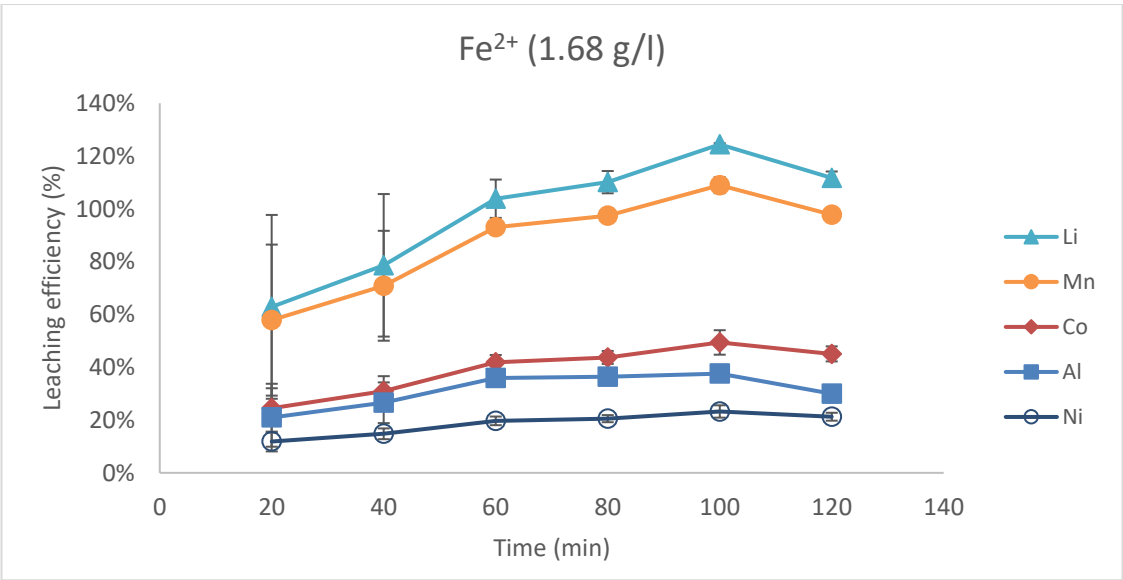

Figure 14. Ferrous ions as catalyst, concentration 1.68 g/l.

In Figure 14 we can see that the optimal leaching efficiency for ferrous ion with concentration 1.68 g/l is achieved after 100 minutes as all of lithium and manganese

were leached, and aluminium, cobalt, and nickel with efficiencies (37.6 %, 49.4 % and 23.2 %).

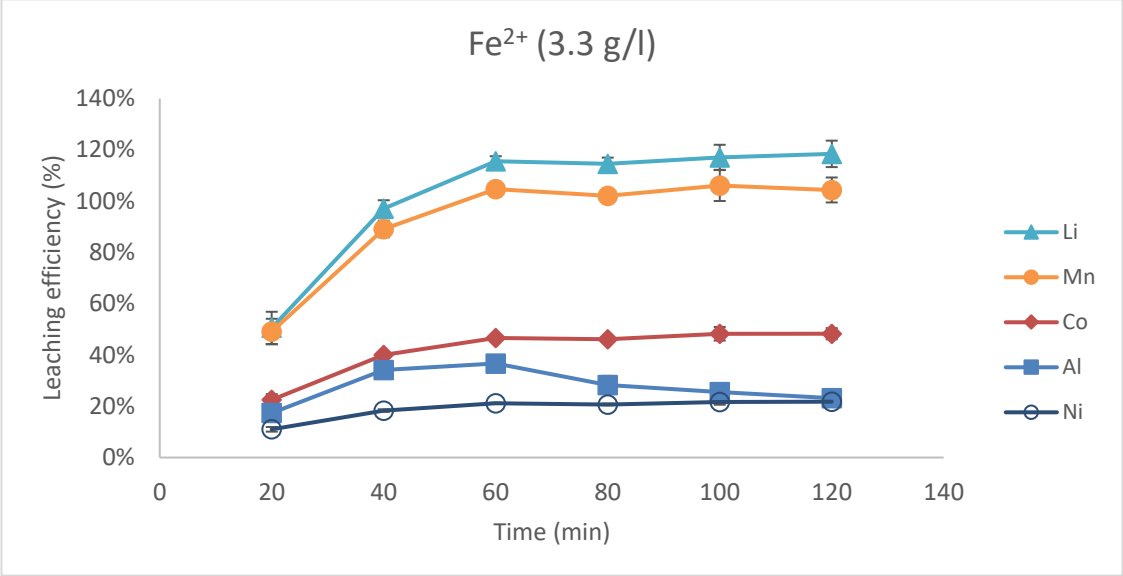

Figure 15. Ferrous ions as catalyst, concentration 3.3 g/l.

In case of ferrous ions as sole catalyst, the concentration of 3.3 g/l reaches the optimal leaching efficiency first with the studied concentrations at 60 minutes: Li, Mn (115.6 % and 104.7 %) and Al, Co, Ni (36.7 %, 46.7 %, 21.1 %), which can be seen in Figure 15.

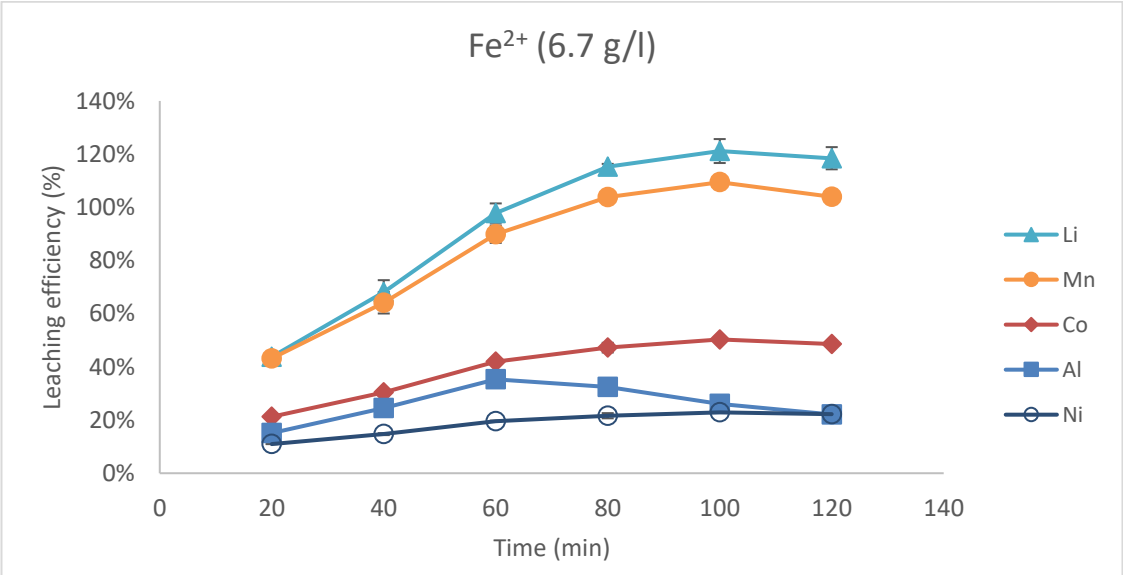

Figure 16. Ferrous ions as catalyst, concentration 6.7 g/l.

Leaching with highest concentration of ferrous ions achieve optimal efficiency at 80 minutes: Li, Mn (115.3 % and 103.8 %) and Al, Co and Mn (32.5 %, 47.2 % and 21.6 %).

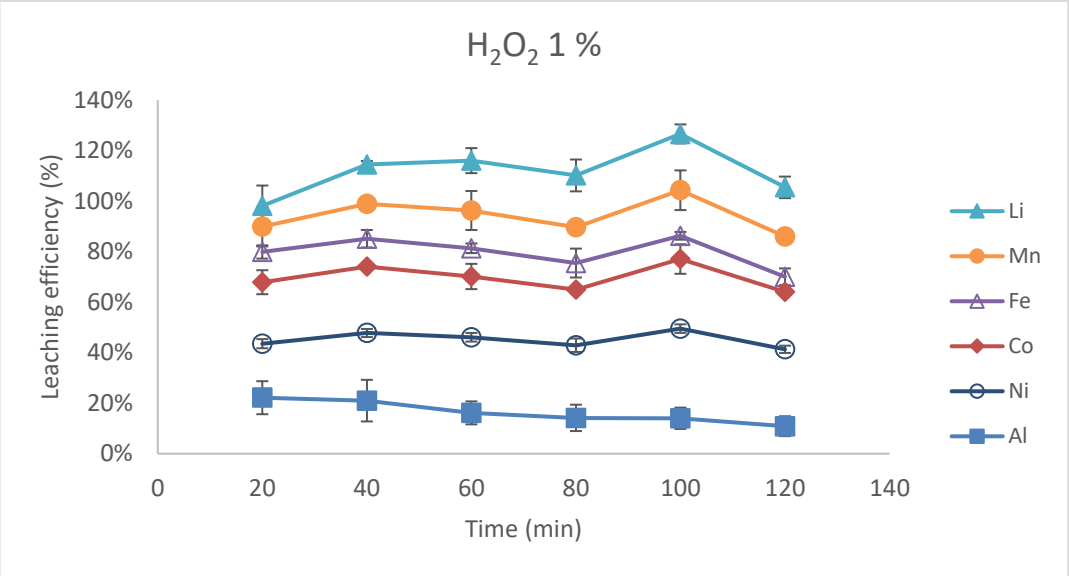

Figure 17. Leaching efficiency with 1 % H_2O_2.

Precipitation of aluminium and iron by hydrogen peroxide can be seen here in Figure 17, at the first time point leachate has 22.2 % aluminium, and 79.9 % iron, whereas in Figure 18 there is 5.6 % of aluminium and 2.9 % iron at the same time point when hydrogen peroxide concentration is increased from 1 % to 5 %.

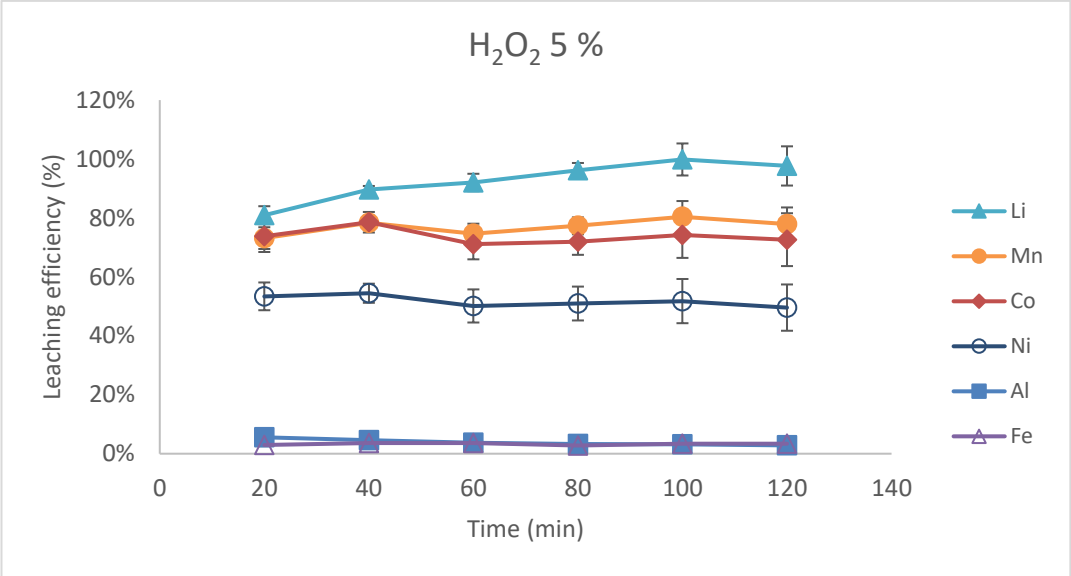

Figure 18. Leaching efficiency with 5 % H_2O_2.

When increasing hydrogen peroxide concentration from 5 % to 10 %, we can only see decreases in leaching efficiency, e.g., leached amount of nickel was decreased from 49.6 % (Figure 18) to 37.2 % (Figure 19) after two hours.

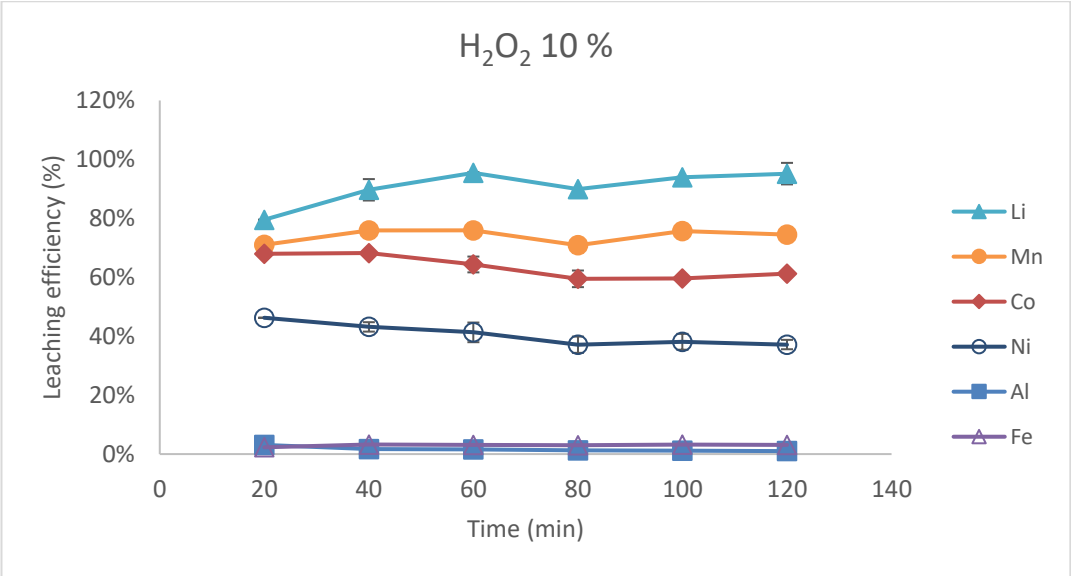

Figure 19. Leaching efficiency with 10 % H_2O_2.

By the results obtained in this experiment, leaching with 1 % H_2O_2 concentration yielded best overall results. Whereas best selectivity would be with ferrous ions concentration of 3.3 g/l.

Combined use of Fe^{2+} and H_2O_2 as catalysts

Only limited studies were available with combined use of hydrogen peroxide and ferrous ions as reducing agents.

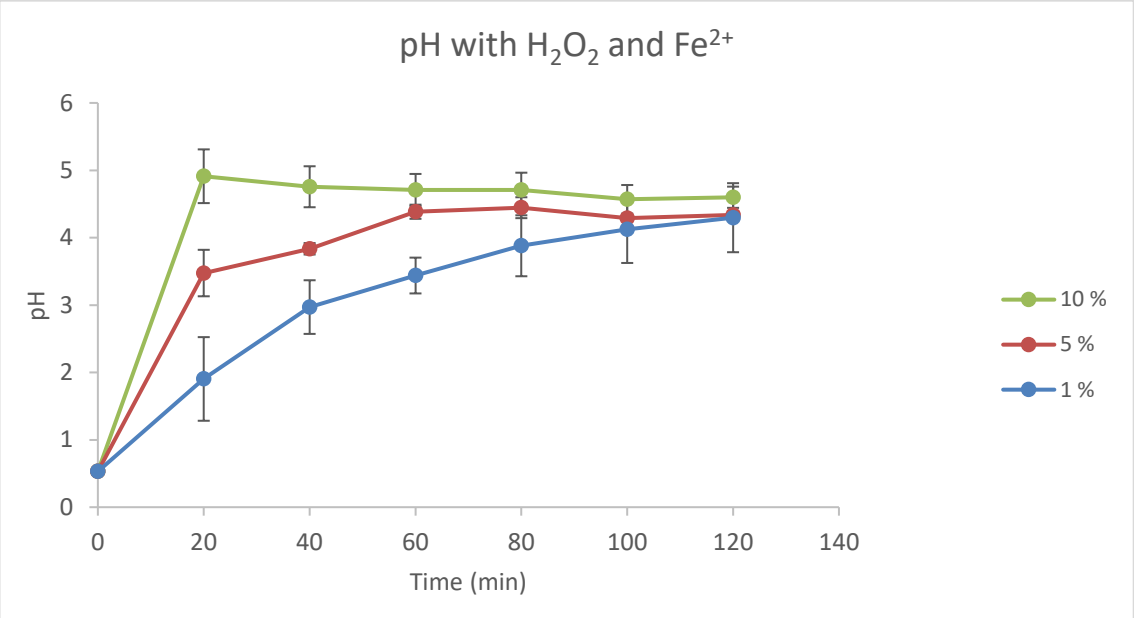

Figure 20. pH with combined use of catalysts.

pH change at the beginning when using both catalysts at the same time Figure 20 follows the same trend as with hydrogen peroxide as sole catalyst (Figure 12), ferrous ions in the same leachate do not seem to have a major effect in pH change.

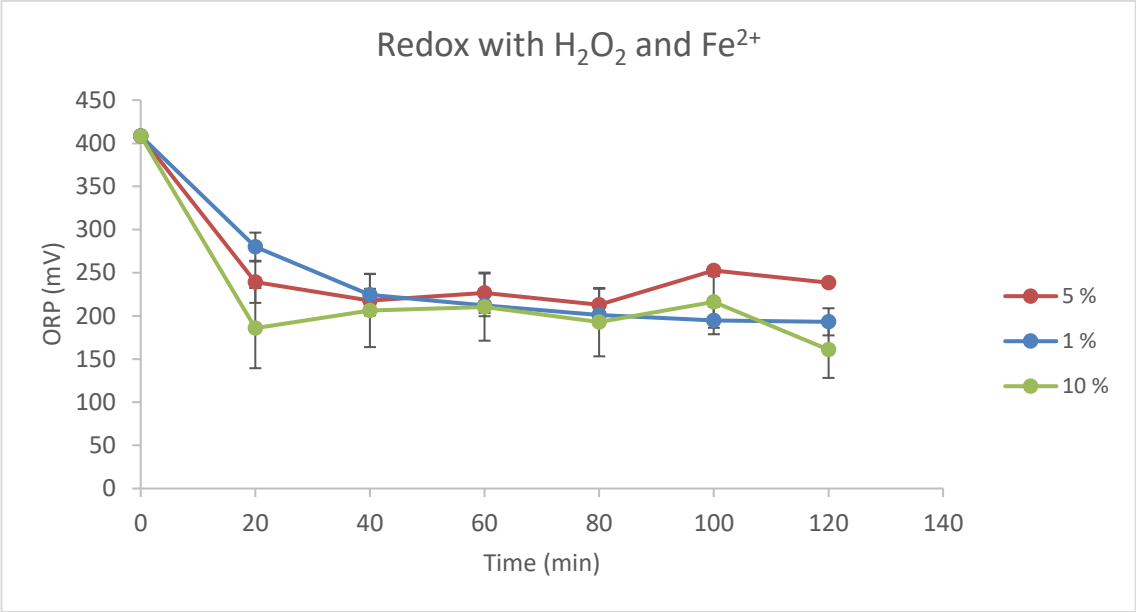

Figure 21. Redox potential change, combined H_2O_2 and Fe^{2+} as catalysts.

Changes in redox potential (Figure 21) mimic the previous results with hydrogen peroxide as shown in Figure 13.

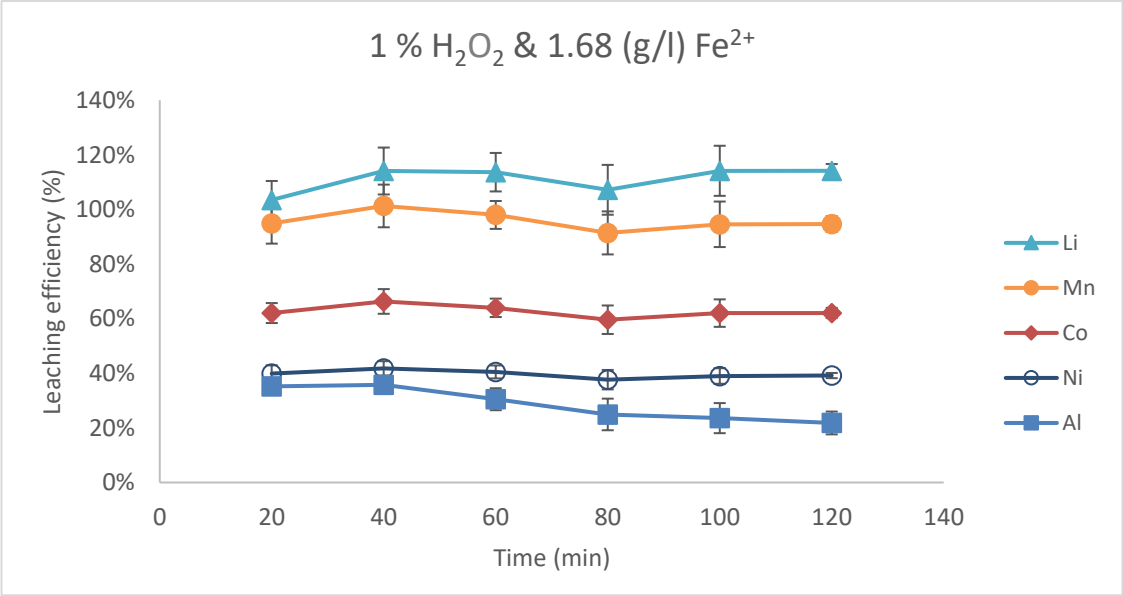

Figure 22. Combined catalyst leaching, 1 % H_2O_2 & 1.68 (g/l) Fe^{2+}.

Peak leaching efficiency is achieved at 40 minutes, shown in Figure 22 with leaching efficiencies Li, Mn (114.1 % and 101.3 %) and Al, Co, Ni (41.8 %, 66.3 % and 41.8 %).

When it comes to combined leaching with both catalysts, setup with lowest concentration (H_2O_2 1 % and Fe^{2+} 1.68 g/l) yielded best results.

When compared to leaching with one catalyst, optimal leaching efficiency was achieved after 40 minutes as it is seen also in Figure 17 and Figure 18, albeit Al, Co and Ni leaching efficiencies are improved with the combination with ferrous ions.

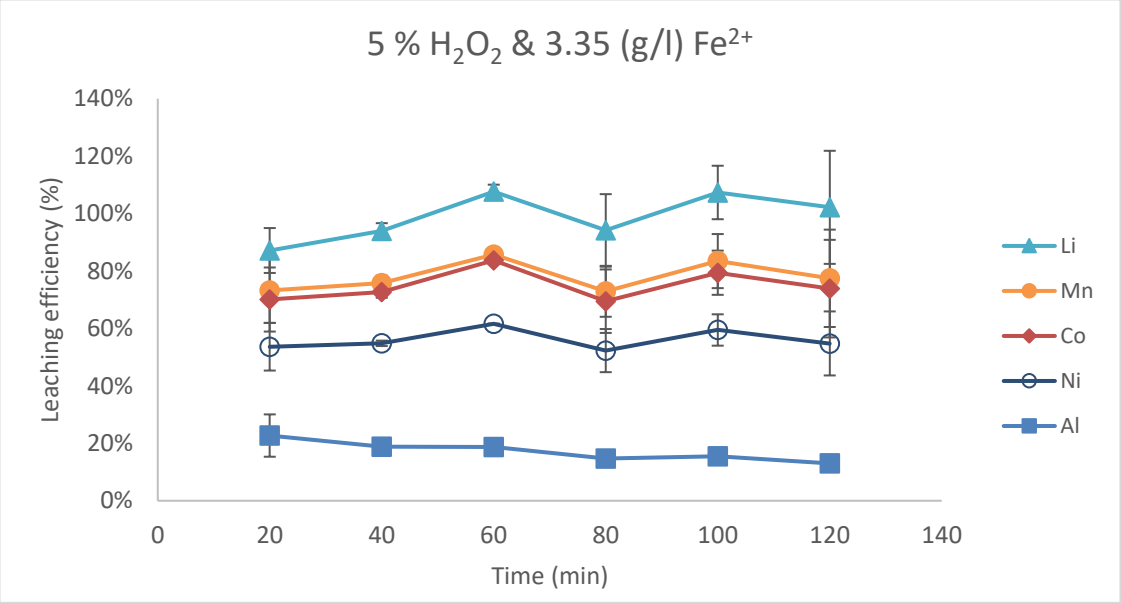

Figure 23. Combined catalyst leaching, 5 % H_2O_2 & 3.35 (g/l) Fe^{2+}.

When increasing the H_2O_2 and Fe^{2+} concentrations simultaneously, which can be seen in Figure 23 and Figure 24 leaching efficiency of nickel increases whereas efficiency decreases with all other metals.

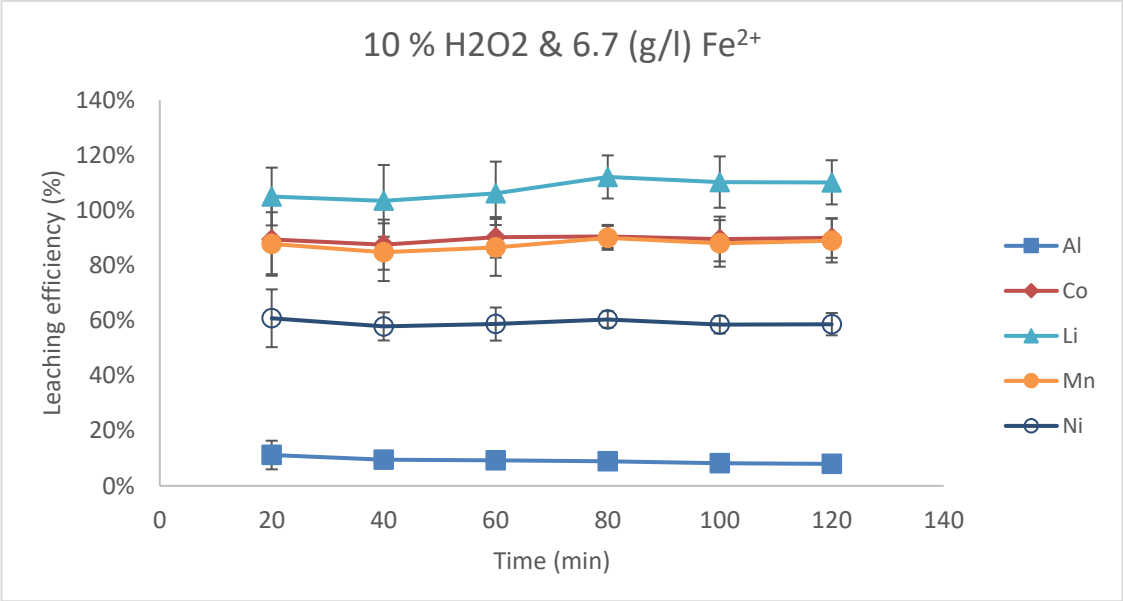

Figure 24. Combined catalyst leaching, 10 % H_2O_2 and 6.7 (g/l) Fe^{2+}.

To leach maximum amount of metals we can conclude from the results that 1 % concentration of H_2O_2 combined with 1.68 g/l Fe^{2+} were the most effective parameters.

Boxall et al. (2018, 509) and Vieceli (2023, 9665) express that sulphuric acid acts as a good leaching agent, which was also observed within all experiments.

Studies by Jha et al. (2013, 1892–1893) and Vieceli et al. (2023, 9664–9668) support the findings of these experiments, that cobalt leaching efficiency is highly affected by the concentration of H_2O_2.

Xin et al. (2016, 254–256), Boxall et al. (2018, 509) and Ghassa et al. (2021, 3–5) demonstrate ferrous ions ability to enhance the leaching efficiency of Co and Ni, which could not be seen in results shown in this chapter. Addition of ferrous ions as sole catalyst did not provide significant increase in leaching time or efficiency and therefore does not make sense as the same leaching efficiency for lithium and manganese can be obtained without ferrous ions. Poor reduction performance of ferrous ions could be explained by lower leaching temperature.

These findings suggest that the pulp density of BM can be increased, even higher than 10 %, room temperature can be used, and short experimental time e.g., 1 hour is possible, at least with the addition of a catalyst e.g, H_2O_2.

5 Conclusion

The purpose of this thesis was to demonstrate the effectiveness of non-contact bioleaching in recycling black mass from spent lithium-ion batteries, specifically the NMC. The research findings indicate that metal leaching efficiency is significantly affected by factors such as pulp density, pH, catalyst and its concentration.

Non-contact bioleaching is an environmentally friendly way to leach waste lithium-ion batteries with higher pulp densities and greater efficiencies without complicated processes, or hazardous and expensive chemicals. This could significantly reduce the toxic waste currently generated due to the alarmingly low recycling of lithium-ion batteries.

The experiments were a success, excellent leaching efficiencies were achieved in significantly shorter periods than expected. Based on the results, we can conclude that non-contact bioleaching can reach commercially appealing pulp densities in a couple of hours. However, more studies are needed to make definitive conclusions due to the low sample size and potential experimental errors.

The use of hydrogen peroxide as a catalyst led to a noticeable increase in cobalt leaching efficiency. However, the use of ferrous ions at room temperature did not show significant changes compared to other leaching setups. The combined use of catalysts yielded the best results, although it might not be economically feasible as the increase from hydrogen peroxide leaching was not major.

It is crucial to thoroughly examine the entire recycling process and identify practical and sustainable recycling techniques. Despite its limitations such as slow acid generation, relatively low pulp densities, and its novelty, non-contact bioleaching shows promise for recycling lithium-ion batteries. Since the chemical composition of batteries varies, it is important to determine the bioleaching acid separately for each process.

Results presented in this thesis demonstrate the capability to reach higher pulp densities, laying the groundwork for further studies. Future research should focus on exploring higher pulp densities, utilizing larger sample sizes, investigating different catalysts, and examining various battery types. Ultrasound-assisted leaching has the potential to reduce leaching time and increase efficiency for nickel leaching, while hydrogen peroxide is a viable and recommendable catalyst, particularly for its efficacy in cobalt leaching.

Additionally, conducting economic studies and implementing process scale-ups are also necessary steps to introduce non-contact bioleaching into the industry and make LIB recycling commercially profitable. These endeavors are crucial for advancing sustainable battery recycling practices and mitigating environmental impacts.

References

Bae, H. & Kim, Y. 2021. Technologies of lithium recycling from waste lithium ion batteries: a review. Materials Advanced. Issue 10. 3234–3250. https://doi.org/10.1039/D1MA00216C

Barshai, A. 2016. Electrowinning 101: What is electrowinning?. EmewCorporation. Accessed on 13 May 2024. https://blog.emew.com/electrowinning-101-what-is-electrowinning

Biswal, B.K. & Balasubramanian, R. 2023. Recovery of valuable metals from spent lithium-ion batteries using microbial agents for bioleaching: a review. Frontiers Microbiology. Sec. Microbiological Chemistry and Geomicrobiology. Vol. 14, 1–25. https://doi.org/10.3389/fmicb.2023.1197081

Bosecker, K. 1997. Bioleaching: metal solubilization by microorganisms. FEMS Microbiology Reviews. Vol. 20, Issue 3-4, 591–604. https://doi.org/10.1111/j.1574-6976.1997.tb00340.x

Boxall, N. J.; Cheng, K. Y.; Bruckard, W. & Kaksonen, A. H. 2018. Application of indirect non-contact bioleaching for extracting metals from waste lithium-ion batteries. Journal of Hazardous Materials. Vol. 360, 504–511. https://doi.org/10.1016/j.jhazmat.2018.08.024

Carlier, M. Electric Vehicles: A global overview A statista report on the electric vehicle market worldwide. Statista. Statista Inc.. Requires login. Accessed on 07 May 2024. https://www-statista-com.ezproxy.turkuamk.fi/study/134904/electric-vehicles-a-global-overview/

Chen, M.; Ma, X.; Chen, B.; Arsenault, R., Karlson, P.; Simon, N. & Wang, Y. 2019. Recycling End-of-Life Electric Vehicle Lithium-Ion Batteries. Joule. Vol. 3, Issue 11, 2622–2646. https://doi.org/10.1016/j.joule.2019.09.014

Cherevko, S. & Mayrhofer, K.J.J. 2017. On-Line Inductively Coupled Plasma Spectrometry in Electrochemistry: Basic Principles and Applications. Encyclopedia of Interfacial Chemistry. Elsevier. 2018. Pages 326–335. ISBN 9780128098943. http://doi.org/10.1016/B978-0-12-409547-2.13292-5.

Council of the European Union 2023. Council adopts new regulation on batteries and waste batteries. Press release. Accessed on 17 April 2024.

https://www.consilium.europa.eu/en/press/press-releases/2023/07/10/council-adopts-new-regulation-on-batteries-and-waste-batteries/

Dobó, Z.; Dinh, T. & Kulcsár, T. 2023. A review on recycling of spent lithium-ion batteries. Energy Reports. Vol. 9, 6362–6395. https://doi.org/10.1016/j.egyr.2023.05.264

Emerson Process Management 2008. FUNDAMENTALS OF ORP MEASUREMENT. Accessed on 19 April 2024. https://www.emerson.com/documents/automation/application-data-sheet-fundamentals-of-orp-measurement-rosemount-en-68438.pdf

European Commission, Directorate-General for Internal Market, Industry, Entrepreneurship and SMEs.; Grohol, M. & Veeh, C. 2023. Study on the critical raw materials for the EU 2023 : final report. Publications Office of the European Union. Accessed on 19 April 2024. https://data.europa.eu/doi/10.2873/725585

Ghassa, S.; Farzanegan, A.; Gharabaghi, M. & Abdollahi, H. 2020. The reductive leaching of waste lithium ion batteries in presence of iron ions: Process optimization and kinetics modelling. Journal of Cleaner Production. Vol. 262, 121312, 1–14. https://doi.org/10.1016/j.jclepro.2020.121312

Ghassa, S.; Farzanegan, A.; Gharabaghi, M. & Abdollahi, H. 2021. Iron scrap, a sustainable reducing agent for waste lithium ions batteries leaching: An environmentally friendly method to treating waste with waste. Resources, Conservation and Recycling. Vol. 166, 105348, 1–10. https://doi.org/10.1016/j.resconrec.2020.105348

Harper, G.; Sommerville, R.; Kendrick, E.; Driscoll, L.; Slater, P.; Stolkin, R.; Walton, A.; Christensen, P.; Heidrich, O.; Lambert, S.; Abbott, A.; Ryder, K.; Gaines, L. & Anderson, P. 2019. Recycling lithium-ion batteries from electric vehicles. Nature. Vol. 575, 75–86. https://doi.org/10.1038/s41586-019-1682-5

He, L.-P.; Sun, S.-Y.; Song, X.-F. & Yu, J.-G. 2017. Leaching process for recovering valuable metals from the $LiNi_{1/3}Co_{1/3}Mn_{1/3}O_2$ cathode of lithium-ion batteries. Waste Management. Vol. 64, 171–181. https://doi.org/10.1016/j.wasman.2017.02.011

Ionode n.d. pH Theory. Accessed on 19 April 2024.https://ionode.com/en/theory/ph-theory

Jha, M. K.; Kumari, A.; Jha, A. K.; Kumar, V.; Hait, J. & Pendey, D. 2013. Recovery of lithium and cobalt from waste lithium ion batteries of mobile phone. Waste Management. Vol. 33, 1890–1897. http://dx.doi.org/10.1016/j.wasman.2013.05.008

Kremser, K.; Maltschnig, M.; Schön, H.; Jandric, A.; Gajdosik, M.; Vaculovic, T.; Kucera, J. & Guebitz, G. M. 2022. Optimized biogenic sulfuric acid production and application in the treatment of waste incineration residues. Waste Management. Vol. 144, 182–190. https://doi.org/10.1016/J.WASMAN.2022.03.0

Levine, M. 2023. ICP-OES – ICP Chemistry, ICP-OES Analysis, Strengths and Limitations. Technology Networks. Accessed on 17 April 2024. https://www.technologynetworks.com/analysis/articles/icp-oes-icp-chemistry-icp-oes-analysis-strengths-and-limitations-342265

Li, J.; Zhang, H.; Wang, H. & Zhang B. 2023. Research progress on bioleaching recovery technology of spent lithium-ion batteries. Environmental Research. Vol. 238, Part 1, 117145. https://doi.org/10.1016/j.envres.2023.117145

Lister, T. E.; Wang, P. & Anderko, A. 2014. Recovery of critical and value metals from mobile electronics enabled by electrochemical processing. Hydrometallurgy. Vol. 149, 228–237. https://doi.org/10.1016/j.hydromet.2014.08.011

Makwarimba, C.P.; Tang, M.; Peng, Y.; Lu, S.; Zheng, L.; Zhao. Z. & Zhen, A. 2022. Assessment of recycling methods and processed for lithium-ion batteries. Cell Press. iScience. Vol. 25, 104321. https://doi.org/10.1016/j.isci.2022.104321

Mettler-Toledo GmbH 2023. pH Theory Guide: A Guide to pH Measurement Theory and Practice of pH Applications. Accessed on 19 April 2024. https://www.mt.com/dam/non-indexed/po/pro/pdf/guides/generic/PA0010en_30078149_pH_Booklet_en_2023_07_LR.pdf

Microscopy Australia n.d. “My Scope-training for advanced research”. Accessed on 16 April 2024. https://myscope.training/#/SEMlevel_3_1

Mining Association of Canada 2021. Projected metal demand growth for battery production worldwide by 2028 (in percent). Statista. Statista Inc.. Requires login. Accessed on 17 April 2024. https://www-statista-com.ezproxy.turkuamk.fi/statistics/665038/projected-growth-in-metal-demand-for-battery-production-worldwide/

O'Driscoll, A. 2023. How SEM/EDS Works and Its Applications in Materials Science. Accessed on 16 April 2024. https://www.labmanager.com/how-sem-eds-works-and-its-applications-in-materials-science-30255

Roy, J.J.; Cao B. & Madhavi S. 2021. A review on the recycling of spent lithium-ion batteries (LIBs) by the bioleaching approach. Chemosphere. Vol. 282, Issue 130944, 1–13. https://doi.org/10.1016/j.chemosphere.2021.130944

Sibananda, S. & Niharbala, D. 2023. Two-step leaching of spent lithium-ion batteries and effective regeneration of critical metals and graphitic carbon employing hexuronic acid. RSC Advances. 13. 7193–7205. http://dx.doi.org/10.1039/D2RA07926G

Statista Market Insights 2023. Revenue in the Electric Vehicles market for different segments Worldwide from 2016 to 2028 (in billion U.S. dollars). Statista. Statista Inc.. Requires login. Accessed on 16 April 2024. https://www-statista-com.ezproxy.turkuamk.fi/forecasts/1444628/revenue-electric-vehicles-market-for-different-segments-worldwide

Tezyapar Kara, I.; Kremser, K. Wangland, S. T. & Coulton, F. 2003. Bioleaching metal-bearing wastes and by-products for resource recovery: a review. Environmental Chemistry Letters. Vol. 21, 3329–3350. https://doi.org/10.1007/s10311-023-01611-4

The Critical Raw Materials Alliance. n.d. Critical Raw Materials. Accessed on 17 April 2024. https://www.crmalliance.eu/critical-raw-materials

United States Environmental Protection Agency (EPA) 2023. Lithium-Ion Battery Recycling. Accessed on 17 April 2024. https://www.epa.gov/hw/lithium-ion-battery-recycling

Vegliò, F.; Quaresima, R.; Fornari, P. & Ubaldini, S. 2003. Recovery of valuable metals from electronic and galvanic industrial wastes by leaching and electrowinning. Waste Management. Vol. 23, 245–252. https://doi.org/10.1016/S0956-053X(02)00157-5

Vernier 2018. The Theory Behind pH Measurements. Accessed on 19 April 2024. https://www.vernier.com/blog/the-theory-behind-ph-measurements/?cn-reloaded=1

Vieceli, N.; Benjamasutin, P.; Promphan, R.; Hellström, P.; Paulsson, M. & Petranikova, M. 2023. Recycling of Lithium-Ion Batteries: Effect of Hydrogen Peroxide and a Dosing Method on Leaching of LCO, NMC Oxides, and Industrial Black Mass. ACS Sustainable Chem. Eng. Vol. 11, 9662–9673. https://doi.org/10.1021/acssuschemeng.3c01238

Xin, Y.; Guo, X.; Chen, S.; Wang, J.; Wu, F. & Xin, B. 2016. Bioleaching of valuable metals Li, Co, Ni and Mn from spent electric vehicle Li-ion batteries for the purpose of recovery. Journal of Cleaner Production. Vol. 116, 249–258. https://doi.org/10.1016/j.jclepro.2016.01.001

ICP-OES sample preparation protocol

Sample preparation for ICP

10 ml samples need to be transferred into 15ml test tubes and spun down at 2500g for 45 minutes and 4°C.

The tubes are subsequently decanted into pellet and supernatant fractions, both in their respective 15ml vial.

For pelleted samples:

1. Samples are overlayed with 200µl of concentrated HNO_3 (Honeywell Fluka, Nitric Acid, Puriss. P.a./ACS Reagent/ Reag. ISO ≥69% - Use this or better quality for preparation, if needed we can provide it)
2. Sample vials are placed in an oven at 60°C o/n with the cap tightly sealed
3. The next day, the vials are taken out and left to cool to RT, before being run for 30 minutes in an ultrasonic bath at 60°C.
4. After sonication treatment, the vials are cooled to RT again, before being filled to 10ml total volume and thoroughly mixed

For supernatant samples:

1. 1ml of supernatant is transferred into a fresh 15ml test tube and mixed with 200µl conc. HNO_3 (similar quality to the reagent mentioned above)
2. Further processing is similar to points: 2., 3., and 4. of the pelleted samples treatment.

The resulting 10ml Samples can be measured up to 3 times.

The ratio of HNO_3 to the total volume in the samples is important for the background accommodation in the spectra and has to be kept constant.

The final DF for the pelleted samples is 1, while the DF for the supernatant samples is 10, but both can be adapted freely, though they need to be shown on the labelling for recalculation on the ICP.